GEODYNAMICS & TECTONOPHYSICS
Published by the Institute of the Earth's Crust, Siberian Branch, Russian Academy of Sciences

PALEOGEODYNAMICS

2023 VOLUME 14 ISSUE 1 ARTICLE 0685

ISSN 2078-502X

DOI: 10.5800/GT-2023-14-1-0685

ON THE TIME AND CONDITIONS OF FORMATION OF THE SHOKSHA QUARTZITE-SANDSTONES OF THE SOUTH ONEGA DEPRESSION BASED ON THE NEW DATA FROM ISOTOPE GEOCHRONOLOGY

N.B. Kuznetsov [1,2]✉, S.Yu. Kolodyazhnyi [1], T.V. Romanyuk [3], A.V. Strashko [1,4], A.S. Baluev [1], E.N. Terekhov [1], S.V. Mezhelovskaya [1,5], A.S. Dubensky [1,4], V.S. Sheshukov [1]

[1] Geological Institute, Russian Academy of Sciences, 7-1 Pyzhevsky Ln, Moscow 119017, Russia
[2] Institute of the Earth's Crust, Siberian Branch, Russian Academy of Sciences, 128 Lermontov St, Irkutsk 664033, Russia
[3] Schmidt Institute of Physics of the Earth, Russian Academy of Sciences, 10-1 Bolshaya Gruzinskaya St, Moscow 123242, Russia
[4] Lomonosov Moscow State University, 1 Leninskie Gory, Moscow 119991, Russia
[5] Sergo Ordzhonikidze Geo University, 23 Miklukho-Maklay St, Moscow 117997, Russia

ABSTRACT. The first results of U-Pb isotope dating of detrital zircons (dZr) from red-colored quartzite-sandstones of the Shoksha Formation (Shoksha horizon) are presented. The Shoksha Formation completes the Vepsian sub-horizon (Vepsian) of the Lower Proterozoic of Karelia and is distributed within the South Onega trough. A sample (KL-555) of red-colored quartzite-sandstones was taken from the lower part of the section of the Shoksha Formation in the same name deposit within the southwestern Onega Lake region. The 79 dZr grains isolated from this sample were analyzed by the staff of the Chemistry-Isotopic Analytic Laboratory of the GIN RAS using the equipment of the Shared Research Facilities of the GIN RAS. The weighted average of the three youngest U-Pb isotope dates for dZr grains is 1906±13 Ma. Taking into account the known isotopic dates of gabbro-dolerites from the Ropruchei sill, that cuts through the Shoksha Formation, it makes possible to constrain the time of the Shoksha Formation accumulation by ~1.90–1.75 Ga. A significant part of the carried out analyzes has yielded a high degree of discordance of the dates. The features of the distribution of the figurative points of these analyzes in the diagram with concordia suggest that the rocks of the studied section of the Shoksha Formation were subjected to the alteration that disturbed the U-Pb isotope system of these zircon grains in the Phanerozoic.

The set of obtained dates for dZr grains has been compared with the known ages of the crystalline complexes of the basement of the East European Platform. The age sets of dZr grains from sample KL-555 and rocks of the Ladoga Group, developed along the margin of the Svecofennian accretionary orogen, are very similar (*p* similarity coefficient in Kolmogorov – Smirnov test is 0.27) and characterize mainly tectonic–magmatic events that had immediately preceded the manifestation of the Svecofennian orogeny (1.9–1.87 Ga). Therefore, the rocks of the Ladoga Group could highly probably be a secondary source for the Shoksha quartzites. Based on a comparative analysis of ages and thorium-uranium ratios (Th/U) in dZr grains from sample KL-555, it was concluded that some of the studied dZr grains with high Th/U>1.5 originate from Ludicovian mafic rocks, but those with low Th/U<0.1 originate from ultra-high-pressure formations, such as eclogites known in the Salma, Kuru-Vaara and Gridino.

A paleo-geographic scheme for the Late Vepsian is proposed, showing that the highly mature Shoksha sandstones were generated under continental conditions in a local basin due to the accumulation of clastic material carried by an extensive and branched sedimentary flow in the direction from north and northwest to south and south-east.

KEYWORDS: Onega Paleoproterozoic structure; Vepsian; Shoksha Formation; detrital zircons; U-Pb dating; paleo-geography

FUNDING: The work has been done as part of the state assignment of GIN RAS and IPE RAS.

RESEARCH ARTICLE

Correspondence: Nikolay B. Kuznetsov, kouznikbor@mail.ru

Received: May 16, 2022
Revised: June 27, 2022
Accepted: July 13, 2022

FOR CITATION: Kuznetsov N.B., Kolodyazhnyi S.Yu., Romanyuk T.V., Strashko A.V., Baluev A.S., Terekhov E.N., Mezhelovskaya S.V., Dubensky A.S., Sheshukov V.S., 2023. On the Time and Conditions of Formation of the Shoksha Quartzite-Sandstones of the South Onega Depression Based on the New Data from Isotope Geochronology. Geodynamics & Tectonophysics 14 (1), 0685. doi:10.5800/GT-2023-14-1-0685

1. INTRODUCTION

Present-day understandings of the Lower Proterozoic stratigraphy of the eastern Baltic Shield (BSh) as a whole and its Karelian province in particular have evolved from the works of K.O. Krats [Krats, 1963]. This stratification was originally based the lithostratigraphic principle and analysis of geological relationships of some lithostratigraphic units with each other and with the Early Proterozoic magmatites. Currently, this stratification is in many cases supported by isotopic-chemostratigrapic correlations with typical Lower Proterozoic cross-section levels [Kuznetsov A.B. et al., 2010, 2011, 2012, 2021; Gorokhov et al., 1998]. Besides, the stratigraphic correlations are confirmed by isotopic ages spatially associated with the Early Proterozoic magmatite supracomplexes [Bibikova et al., 1990; Lubnina et al., 2012]. The present-day understanding of the Lower Proterozoic stratigraphy of the eastern BSh is best reflected in [Negrutsa, 2011] and presented in App. 1, Table 1.1.

Despite significant advances in the study of the Precambrian Karelian province and its adjacent structures, there are not too many reliable chemostratigraphic correlations and isotope ages. For this reason, some problems of detailing the stratigraphic scheme and correlation of the Lower Proterozoic of this region still remain unsolved. These schemes have continued to be improved [Kulikov et al., 2017a, 2017b; Kuznetsov A.B. et al., 2021].

The upper part of the cross-section of the Lower Precambrian Karelia-Kola region [Negrutsa, 2011] consists of the red quartzitic sandstone unit – the Shoksha Formation. Its spreading area is located in the southern Karelia, south-western Cis-Onega. The Shoksha Formation comprises the upper part of the layered complex section whose lower part consists of gray terrigenous rocks of the Petrozavodsk (Kamennoborsk) Formation unconformably overlying typical Lower Proterozoic formations (Karelides). Unlike the Karelides, the rocks of the Petrozavodsk and Shoksha Formations underwent epigenetic tectonometamorphic transformations to a much lesser degree. The Shoksha Formation, in turn, is unconformably overlain by the Upper Vendian sediment cover of the Russian plate.

Such details of relationships with the underlying and overlying formations has long allowed assigning the layered complex of the Petrozavodsk and Shoksha Formations to the Jotnian (the Middle Riphean within the Karelia) [Galdobina, 1958; Galdobina, Mikhailyuk, 1966, 1971; Garbar, 1971; Perevozchikova, 1957; and others]. These formations were then ranked as the same name horizons combined into the Vepsian sub-horizon [Negrutsa, 1984]. The age limits for the Vepsian sub-horizon formation have been in question for quite a long time and are not reliably determined so far. The upper age limit for the Vepsian is based on the fact that the Shoksha Formation is cut through by gabbrodolerite sills which yielded the U-Pb isotopic ages of 1.77–1.75 Ga (1770±12 Ma by zircon, 1751 ±3 Ma by baddeleyite) [Bibikova et al., 1990; Lubnina et al., 2012].

The Shoksha Formation is composed of red quartzite-sandstones with unique decorative characteristics. This bedrock only occurs in Cis-Onega. The boulder-shaped rocks occur in the Quaternary moraines of the Middle Russia. In Saint-Petersburg, the Shoksha quartzites were used for coating of the Saint Isaac's and Kazan cathedrals, in Moscow – for coating of the Cathedral of Christ the Saviour, steles of Hero-Cities and Cities of Military Glory, and the Tomb of the Unknown Soldier in the Alexander Garden. The Shoksha quartz sandstones were also used to make a significant portion of the elements of Lenin's Mausoleum and Napoleon's tomb in the Paris Invalides.

In the last decades, the geological studies are actively conducted using U-Pb isotopic dating of detrital zircon grains (dZr) from the clastic rocks. This made it possible to obtain reliable data on the age of the crystalline (magmatic, metamorphic, hydrothermal and other) complexes which were the primary sources of dZr grains for the units studied.

Direct geochronological data on the ages of the crystalline complexes within some of the regions and the age datasets on dZr grains from the heterochronous clastic sedimentary rocks, occurring in the areas adjacent to the areas where these crystalline compleses are located, complement each other. The dZr grains from the ancient clastic rocks can contain information on the complexes which vanished in the process of geological evolution (completely eroded, completely metamorphically/metasomatically reworked, disappeared in the subduction zones etc.). The onetime existence of these complexes cannot now be proved by other methods.

The comparison between the age datasets on dZr grains from the heterochronous clastic sedimentary rocks in the same area allows tracing the evolution of supplying provinces in time. This provides the possibility of testing the existing paleogeographic and paleotectonic models. The age of a group of the youngest dZr grains with an allowable analytical error and an acceptable discordance level can sometimes be used to determine the lower limit on the age of sediment from which the studied sample has been taken.

By now, some Proterozoic clastic sedimentary rocks of the East European Platform (EEP) and its northeast-bordering structures have already been characterized by the data on the distribution of dZr grain ages, thereby indicating a possibility of further refinement of the stratigraphic position and age of the sediments studied, making stratigraphic correlations, and testing the paleotectonic and paleogeographic evolution models for these regions. The paper presents the first results on U-Pb dating of dZr grains from the red quartz sandstones of the Shoksha Formation of the South Onega trough. The age dataset obtained for dZr grains has been compared with the ages obtained for different Archean–Early Proterozoic crystalline complexes of the BSh and Fennoscandian part of the EEP basement, and with the U-Pb age datasets on dZr grains from the clastic rocks of the Riphean sediments of the EEP and its bordering folds (Fig. 1).

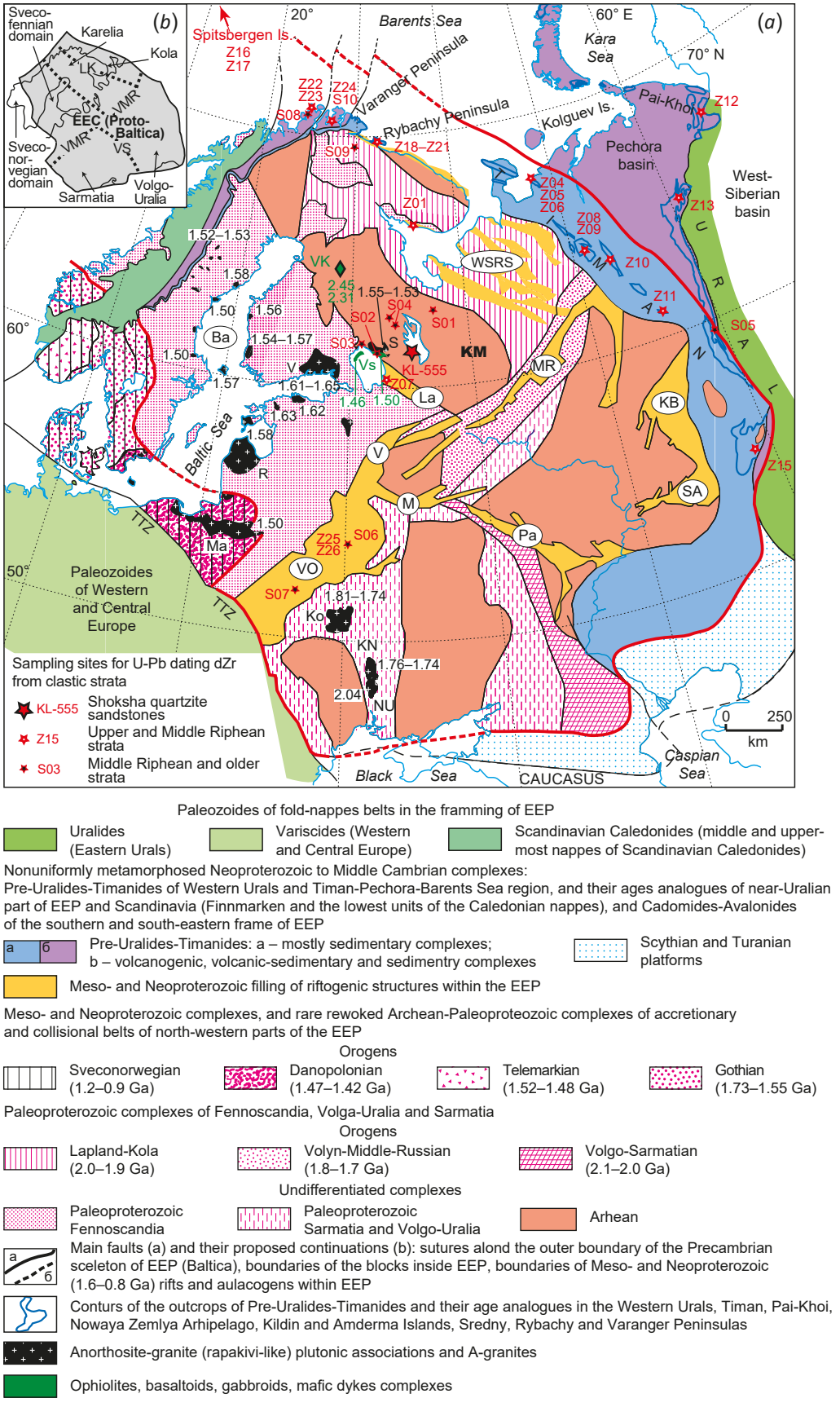

Fig. 1. Tectonic scheme of the basement of the East European Platform (EEP) and its framing structures indicating the sites of sampling from the clastic sediment rocks for which U-Pb dating of detrital zircons has been performed.
The boundary of the ancient basement of the EEP – red line; age of magmatites (Ga) – numbers in black. TTZ is the Teisseyre-Tornquist zone (Trans-European Suture Zone). KM – Karelian massif. Aulacogenes and grabens (inscriptions in circles): MR – Middle-Russian,

VO – Volyn-Orsha, Pa – Pachelma, KB – Kama-Belaya, SA – Sernovodsk-Abdulino, M – Moscow, B – Valdai, La – Pasha-Ladoga, Ba – Baltic-Bothnian (under water), WSRS – Rift System of the White Sea. Plutons: Ko – Korosten, KN – Korsun-Novomirgorod (after [Shumlyansky et al., 2017]), NU – Novo-Ukrainian (after [Stepanyuk et al., 2017]), Ma – Mazura, R – Riga, V – Vyborg, S – Salmi [Larin, 2009, 2011; Sharov, 2020]. Vs – Valaam sill (after [Ramo et al., 2001]), VK – basites composing dykes near Lake Verhnee Kuito (after [Stepanova et al., 2014b]). Inset: Scheme of the domains of the East European Craton (EEC) and the orogens that sutured them (LK – Lapland-Kola, VS – Volgo-Sarmatian, VMR – Volyn-Middle Russian).

2. GENERAL INFORMATION ABOUT THE STRUCTURE OF THE KARELIAN PROVINCE OF THE BALTIC SHIELD

The Karelian massif (KM), often referred to as the Karelian craton in recent publications [Mints et al., 2004; Lubnina, Slabunov, 2017], is situated in the southeastern part of the Baltic Shield. Southwest of the KM, there occur the relics of the Early Proterozoic Svecofennian accretionary orogen (Fig. 2) and northeast of it – the Archean-Proterozoic formations of the Belomorian-Lapland (Kola-Lapland) mobile belt [Morozov, 2010; Kulikov et al., 2017b; Daly et al., 2006; Lahtinen, Huhma, 2019].

The Karelian massif has a clearly defined two-membered upper crustal structure. The lower structural level involves the Archean complexes of granite and gneiss domes and greenstone belts which form extended relatively narrow zones elongated primarily in the submeridional direction [Kozhevnikov, 2000; Kulikov et al., 2017b; Miller, 1988]. The Archean granite-greenstone basement of the KM is unconformably overlain by the formations of the upper structural level which is generally characterized as a proto-platform cover consisting of the Lower Proterozoic volcanogenic and sedimentary materials. These materials and their paragenetically related intrusions of contrastingly differentiated magmatic series were formed in the intra-plate environments of scattered (diffuse) rifting which occurred in relation to the development of plumes whose maximum activity is confined to the time intervals from 2.53–2.42 to 2.1–1.95 Ga [Sokolov, 1987; Kulikov et al., 2017a, 2017b; Stepanova et al., 2014b, 2017, 2020; Mints, Eriksson, 2016].

The Early Proterozoic sedimentary and volcanogenic materials of the proto-platform cover, overlying the Archean granite-greenstone basement of the southern KM, compose the Onega synclinorium. The proto-platform cover cross-section displays a number of geological subdivisions – formations, series or horizons (Fig. 3) combined into 6 sub-horizons (from bottom to top): Sumian, Sariolian, Jatulian, Lyudikovian, Kalevian and Vepsian [Krats, 1963; Negrutsa, 2011; Kulikov et al., 2017a, 2017b; Lower Precambrian Stratigraphic Scale, 2002; and others].

The **Sumian sub-horizon** (2500–2400 Ma) at basement level is composed of thin weathering crusts and highly mature siliciclastic formations. They are overlain by volcanic rocks, primarily andesibasalts, with the thickness of up to 1.5 km. The volcanics compose the relics of the rift system formed at the very beginning of the Early Proterozoic. These formations can still be found in local graben-shaped structures near the Onega synclinorium and form a wide belt along the northeastern margin of the KM. The intrusive complexes – comagmates of their related volcanics – occur both in the KM, and Belomorian province. These are often layered mafite-ultramafite massifs; the largest of which – Burakovka massif (~630 km^2) – lies northeast of the Onega synclinorium and comprises chromite-hosted inclusions [Glushanin et al., 2011]. The Sumian sub-horizon, together with its overlying Sariolian sub-horizon (see below), composes the proto-plate part of the proto-platform cover of the KM and makes up the graben-shaped structures (Fig. 3).

The **Sariolian sub-horizon** (2400–2300 Ma) is usually represented by polymictic conglomerates and conglomerate-breccias. Except for conglomerates, conglomerate-breccias and sandstones, in the upper cross-section revealing the Sariolian along the northeastern and northern margins of the KM there are also exhibited andesibasalts [Korosov, 1991]. The Sariolian formations are spatially related to rifting structures and volcanics of the Sumian and, jointly with them, compose the proto-plate part of the proto-platform cover of the KM and make up the graben-shaped structures (Fig. 3).

The **Jatulian sub-horizon** (2300–2100 Ma) is comprised of volcanogenic and sedimentary materials of alternating thickness (from the first meters to 2 km) whose bottom cross-section consists of areally distributed silicate crusts of chemical weathering. The Jatulian composes the bottom section of the plate part of the proto-platform cover of the KM, overlies with a sharp, angular unconformity the Sumian-Sariolian units and beyond them lays directly on the KM Archean crystalline basement rocks (Fig. 3). Nearly half of the Jatulian formations are lavas. The Jatulian cross-sections have three-membered structure: Lower, Middle and Upper Jatulian whose bottom parts comprise terrigenous and/or terrigenous and carbonate rocks and the top parts consist of volcanogenic formations [Sokolov, 1987]. The Lower Jatulian cross-sections are dominated by terrigenous sedimentary rocks, the Middle Jatulian cross-sections – by terrigenous and carbonate rocks, and most of the Upper Jatulian cross-section is composed of carbonate sediments including bioherms [Makarikhin, Kononova, 1983]. The Onega parametric borehole drilled in the Jatulian basement deposits, overlying the Archean basement rocks, has penetrated evaporates – predominantly halites, as well as anhydrites and magnesites (depth interval 2944.0–2750.8 m) [Glushanin et al., 2011]. The Jatulian rocks were accumulated in the shallow epi-platform basin that had occupied almost the whole area of the KM [Heiskanen, 1990, 1996]. The Jatulian volcanics are the products of fissure eruptions occurred in the intra-plate (intra-platform) environments. They formed an extensive basaltic plateau

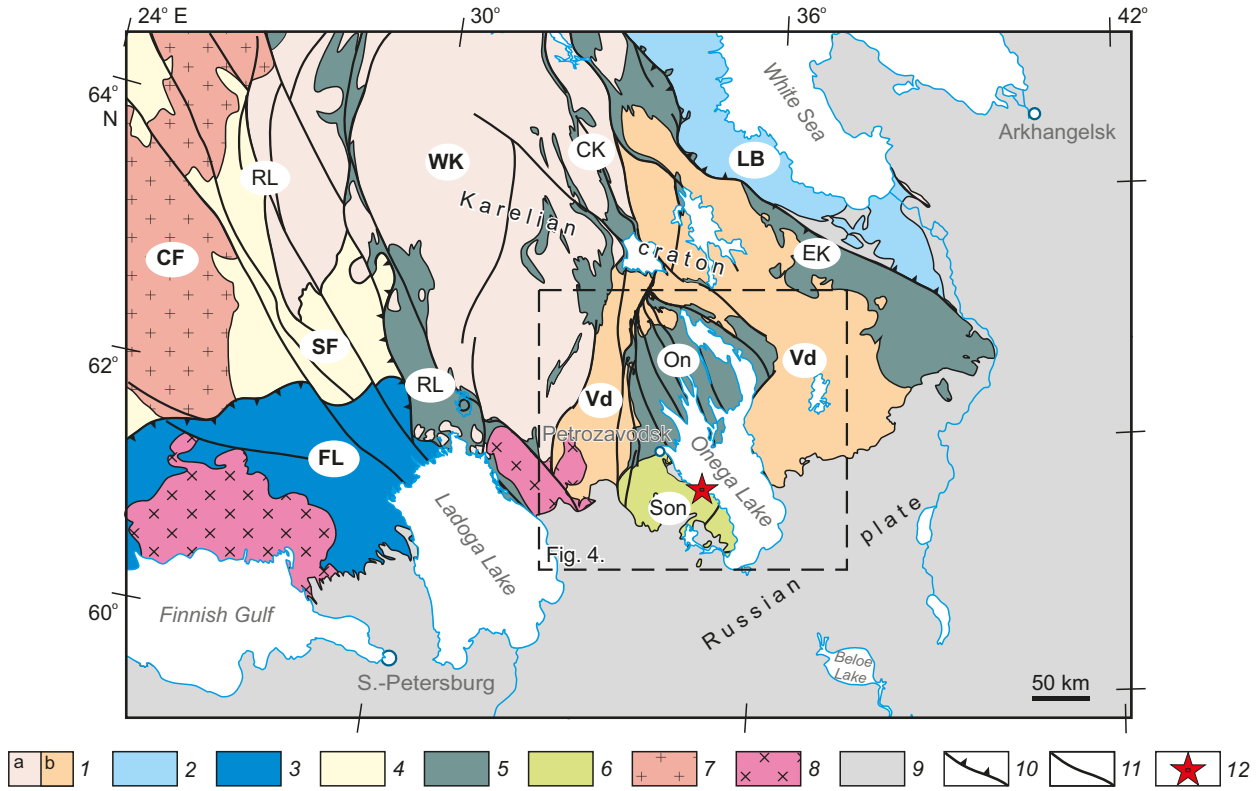

Fig. 2. Scheme of the geological structure of the south-eastern part of the Baltic Shield (used [Morozov, 2010; Kolodyazhny, 2006; Kulikov et al., 2017b]).
1 – Archean granite-greenstone complexes: a – of the West Karelian (WK), b – of the Vodlozersk (Vd) massifs; *2* – Archean – Lower Proterozoic granulite-gneiss complexes of the Lapland-White Sea Belt (LB); *3–7* – Lower Proterozoic complexes: *3* – metamorphic and igneous of the South Finnish-Ladoga Belt (FL), *4* – volcanogenic-sedimentary and igneous island – arc of the Svekofennian belt (SF), *5* – volcanogenic-sedimentary rift and marginal continental complexes of the Karelian massif, *6* – terrigenous deposits of the South Onega depression, *7* – granitoids of the Central Finnish massif (CF); *8* – Early Riphean rapakivi granites; *9* – Vend – Phanerozoic cover of the East European Platform; *10–11* – faults: *10* – thrusts, *11* – mainly strike-slip; *13* – sampling site KL-555. Shear zones: RL – Raakhe-Ladoga, CK – Central Karelian, EK – East Karelian; On – Onega synclinorium, Son – South Onega synclinorium.

similar to the Phanerozoic traps. Volcanism occurred thrice, at the end of each transgressive-regressive cycle, which meets the ideas of the occurrence of major stages of volcanic eruption in young trappean provinces against the background of transgressive tectonics and marine regression [Svetov et al., 2015].

The **Lyudikovian sub-horizon** (2100–1920 Ma) is composed of originally clay, carbonate, strongly carboniferous rocks and volcanics. In the Onega synclinorium, the Lyudikovian sub-horizon comprises the Zaonega and Suisar Formations (horizons). The Zaonega Formation (1.3 km thick) is composed of shungites, shungite-bearing tufoaleurolites, argillites, silicites, limestones and dolomites, containing a large amount of mafic magmatic rock beds. The Suisar Formation (650 m in thickness) is comprised of tuffs and pyroxene, plagioclase and picrite basalt lavas.

The **Kalevian sub-horizon** (1920–1800 Ma) in the Onega synclinorium is composed of monotonously alternating aleurites, clay schists, arkose and quartz sandstones, and locally occurring gravellites, silicites and acid tuffites. This section of flyschoids, most widespread along the southwestern margin of the KM (Ladoga Group), is as thick as 10000 m.

The **Vespian sub-horizon** (1800–1750 Ma) combines the Petrozavodsk (lower) and Shoksha (upper) Formations (horizons) [Sokolov, 1987]. The Petrozavodsk Formation is composed predominantly of gray laminated arkose sandstones, aleurolites and argillites, rarely conglomerates, with a total thickness of more than 300 m [Galdobina, Mikhailyuk, 1971]. The cross-section displays the breccia interlayers with shungite schist and volcanic rock fragments. The Shoksha Formation (horizon) lying unconformably on the Petrozavodsk Formation at the section bottom is composed of red sandstones and quartzite-sandstones with conglomerate lenses. The formation is no thinner than 1000 m. The sandstones and quartzite-sandstones of the Shoksha Formation are composed of mature, mainly quartz fragments and characterized by crimson, red or pink color due to dispersed iron oxides (hematite) in cement, obliquely layered stratification within some series, and evidence of ripples, raindrop impacts and mud cracks on bedding surface, and a high facial variability as a whole. These features are indicative of arid continental depositional environment [Galdobina, 1958; Galdobina, Mikhailyuk, 1966, 1971; Vigdorchik et al., 1968; Garbar, 1971; Sokolov, 1987]. There was found in the bottom section

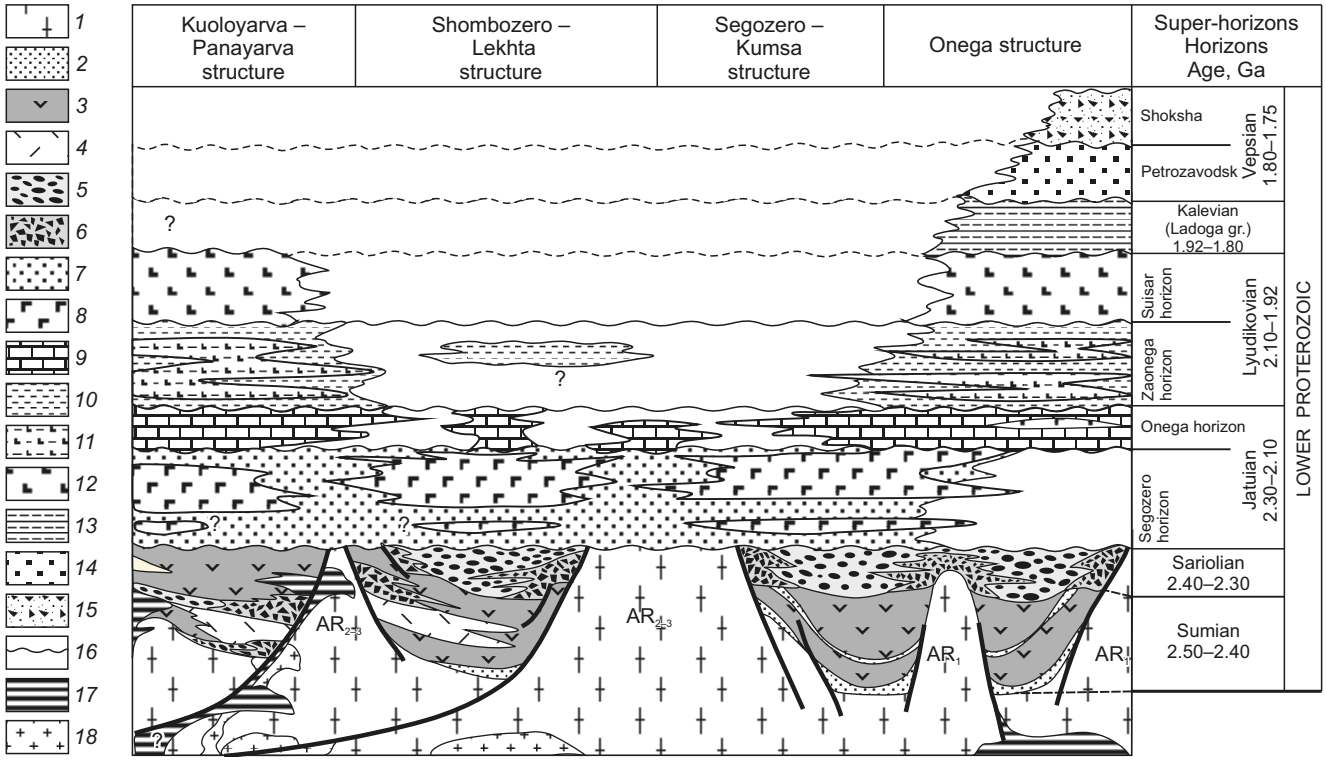

Fig. 3. Generalized lithostratigraphic section of the proto-platform cover of the Karelian massif (after [Kolodyazhny, 2006; Korosov, 1991; Kulikov, 1999; Kulikov et al., 2017a, 2017b; Makarikhin et al., 1995; Sokolov et al., 1970; Sokolov, 1984; Systra, 1991; Kharitonov, 1966; and others].

1 – Archean basement of the Karelian massif (craton); *2–15* – proto-platform cover of the Karelian massif: *2–6* – proto-plate (rifting) part of the proto-platform cover – Sumian and Sariolian: *2* – weathering crusts and terrigenous sediments, *3* – andesite basalts, *4* – quartz and plagioclase porphyries, *5* – polymictic conglomerates, *6* – block breccias and mixtite-like formations; *7–15* – a plate part of the proto-platform cover: *7–9* – Jatulian: *7* – terrigenous rocks, *8* – flood basalts, *9* – carbonate-terrigenous rocks; *10–12* – Lyudikovian: *10* – shungite shales, *11* – basalt lavas, lavobreccia, tuffs, *12* – picrobasalts; *13* – Kalevian: terrigenous flyschoid and molassoid sediments; *14–15* – Vepsian: *14* – terrigenous molassoid formations, *15* – red-colored terrigenous (Shoksha) sandstones; *16* – unconformities; *17* – stratified mafic-ultramafic intrusions (2.44 Ga); *18* – microcline granites (2.44–2.45 Ga).

of the Shoksha Formation a thin (10 m) cover of hematitized basalts [Svetov, 1979].

The results of basin and facial analyses of the Vepsian formations showed that during this complex sediment deposition there was a gradual decrease and shallowing in the paleobasin area to the South Onega trough [Akhmedov et al., 2004; Galdobina, 1958; Galdobina, Mikhailyuk, 1971].

3. TECTONICS OF THE ONEGA SYNCLINORIUM AND ITS FRAMING

The Onega synclinorium is located in the southeastern part of the KM within the Vodlozero block (domain) which represents the oldest Early Archean granite-gneiss core of the KM (Fig. 4) and represents the oldest Early Archean granite-gneiss core of the KM [Kozhevnikov, 2000; Kozhevnikov et al., 2006, 2010; Kozhevnikov, Skublov, 2010; Kulikov et al., 1990, 2017a, 2017b; Levchenkov et al., 1989; Lobach-Zhuchenko et al., 1989, 2000, 2009; Puchtel et al., 1991; Sergeev et al., 2007; Chekulaev et al., 2009a, 2009b]. The Vodlozero domain has conditional borders determined from the location of the Mesoarchean (Lopian) marginal greenstone belts.

The Onega synclinorium comprises two structurally isolated negative structures – North Onega and South Onega basins. The North Onega basin is composed of the formations of the lower and middle parts of the Lower Proterozoic (Sumian, Sariolian, Jatulian, Lyudikovian and Kavelian strata), and the South Onega basin – of the formations of the upper part of the Lower Proterozoic (Vepsian) (Fig. 4). The North Onega and South Onega basins have delta-shaped and oval contours, correspondently. They are located in the area of fan-shaped branching of the northwest striking Central Karelian shear zone; the branches are bordering the basins and complicate their inner structure [Kolodyazhny, 2006; Glushanin et al., 2011].

The Sumian andesibasalts and Sariolian conglomerates in the North Onega basin are localized in the rift graben-shaped structures whose fragments are exposed on the western and northeastern basin sides. Among the Archean gneisses bordering the North Onega basin on the east there is the large stratified mafic Burakovka massif (Br in Fig. 4) and related dyke swarms which are considered as a deep-seated structural element of the Sumian rift system [Glushanin et al., 2011].

The main feature of the North Onega basin structure is an alternation of wide trough-shaped synclines and narrow linear ridge-like anticlines localized in fault zones

[Glushanin et al., 2011]. The Jatulian and Lyudikovian carbonate-terrigenous layers deposited in the cores of the anticlines are much thicker than those deposited in the cores of the conjugate synclines and the fold-close flanks. This is indicative of tectonic layer-wise low viscosity rock flow with pressure-driven rock movement towards the anticline hinges which sometimes leads to the fact that the cores of the anticlines develop a diapir-like structure. The fold axes show virgation and undulation but are oriented northwest as a whole.

The core structure of diapir-like anticlines involves the rocks of the lower parts of the Lower Proterozoic including salt-bearing units similar to that penetrated by the parametric borehole in the base of the Onega synclinorium cross-section. Besides, dispirism sometimes involves the Archean granite-gneisses of the KM basement. The degree of structural and material reworking of rock in the anticlinal zones is very large due to folding and faulting. Such style peculiar to the syn-Svecofennian deformations (1.90–1.87 Ga) is only typical of the North Onega basin. Schistosity, cataclasis and brecciation occurred therein are sometimes associated with intensive metasomatic albite-carbonate-mica mineralization. K-Ar ages obtained on this mineralization display the value ranges of 1900–1700, 1100–900, 150–100 Ma [Polekhovsky et al., 1995].

The Archean rocks, directly bordering the North Onega basin, form different-rank dome-shaped and lenticular structures describing the half-closed belt. A large Archean basement protrusion – the Unitsky dome (Un in Fig. 4) – complicates the northern centroclinal of the basin. There were identified features of an active growth of the marginal dome-shaped structures in the end of the Archean, Paleoproterozoic, and at the present-day stage of development [Kolodyazhny et al., 2000; Glushanin et al., 2011].

The folded structures complicating the inner structure of the North Onega basin on the southwest are with a sharp, angular unconformity overlain by the Vepsian units of the South Onega basin (Son in Fig. 4). This basin is less complex in structure [Garbar, 1971; Sokolov, 1987; Glushanin et al., 2011], oval-contoured, occupies an area of 9000 km^2 and extends over 120 km southeast of Petrozavodsk, reaching 50–70 km in width. On the eastern flank of the South Onega basin, the rocks dip gently, at an angle of 10–12°, rarely 20–25°; on the western flank, the dip gives a steeper angle of descent of the rocks relative to a horizontal plane and reaches 70° in the near-fault zones. In the central part of the basin the rocks lie almost horizontally.

The inner structure of the South Onega basin is complicated by the NW- and NE-striking faults. Using the geophysical data as a base, in the central part of the basin there was identified the northeast-oriented zone considered as a continuation of the Burakovka-Kozhozero deep-seated zone controlling the location of large mafic intrusions [Glushanin

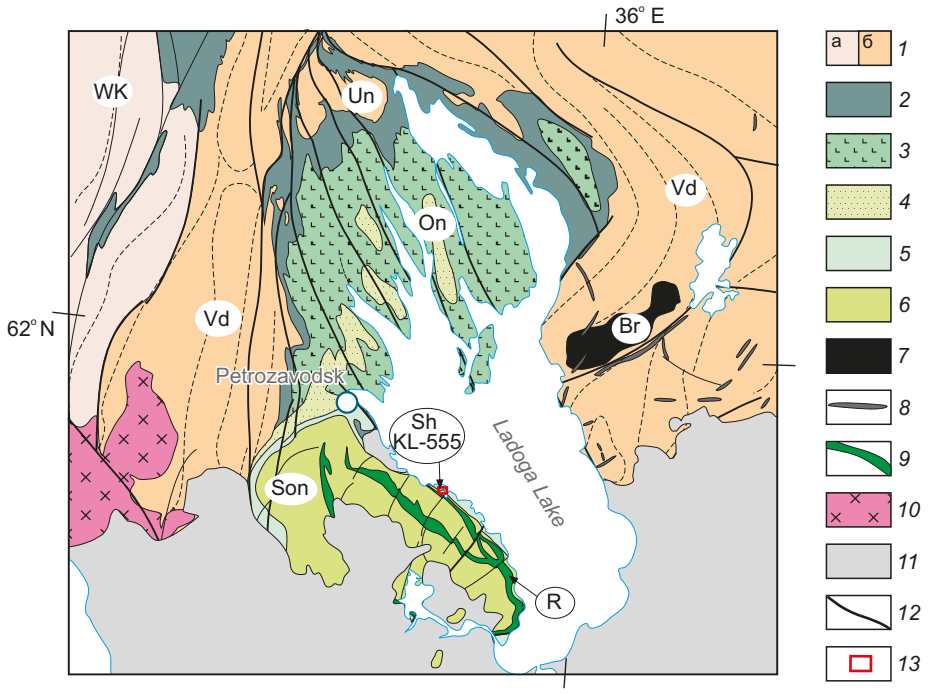

Fig. 4. The structural-geological scheme of the Onega synclinorium (with changes according to [Voitovich, 1971; Kolodyazhny, 2006; Glushanin et al., 2011; Systra, 1991]).
1 – Archean granite-greenstone complexes: a – West Karelian (WK), b – Vodlozersk (Vd) massif; *2–9* – Lower Proterozoic complexes: *2* – Sumian, Sariolian and Jatulian, *3* – Ludikovian, *4* – Kalevian, *5* – Vepsian Petrozavodsk Formation, *6* – Vepsian Shoksha Formation, *7* – mafic-ultramafic stratified massifs, *8* – dykes of basites, *9* – sills of gabbro-dolerites; *10* – Early Riphean rapakivi granites; *11* – Vend – Phanerozoic cover; *12* – faults; *13* – Shoksha quartzite-sandstones deposit (sampling site KL-555). Vd – Vodlozersk block, WK – West Karelian block, On – Onega synclinorium, Son – South-Onega synclinorium, Un – Unitsk dome, Br– Burakovka intrusion, Sh – Shoksha deposit of quartzite-sandstones.

et al., 2011; Ryazantsev, 2012, 2014]. The formation of the South Onega basin is related to final episodes of the Karelian tectonic era when there occurred a transition from the Svecofennian (1.9–1.87 Ga) folding to a relatively quiet proto-platform tectonic regime [Systra, 1991].

The upper sections of the Vepsian strata in the South Onega basin (Shoksha Formation) are intruded by gabbro-dolerite sills of the Ropruchei complex. The largest, Ropruchei sill has an extending 100 km along the southwestern coast of Lake Onega (Fig. 4). It consists of three bodies connected to each other by links. The main body 80–200 m in thickness is primarily composed of middle-grained gabbro-dolerites and gabbro, and the other two bodies (overlying and underlying), with a thickness of up to 25 m, are represented by dolerites, including small-grained, sometimes with an amygdaloidal structure in near-contact parts. Some researchers interpret them as lava flows [Glushanin et al., 2011]. The U-Pb isotopic ages by zircon and baddeleyite from gabbroids of the sill are 1770 ±12 Ma and 1751±3 Ma, respectively [Bibikova et al., 1990; Lubnina et al., 2012].

4. THE STRUCTURE OF THE SHOKHA FORMATION AND LITHOLOGICAL FEATURES OF ITS CONSTITUENT ROCKS

The first scientific information on red sandstones of the Olonets province in Cis-Onega region appeared in the late XVIII – early XIX centuries. These were the descriptions of some outcrops made by S. Alopaeus, N.Ya. Ozeretskovsky, K.M. Arsentyev, A.A. Foullon and I. Engelmann. R. Murchison assigned them to the Devonian on the basis of their similarity with the Old Red Sandstones in England. However, as long as G.P. Helmersen asserted that the Cis-Onega sandstones could be distinguished as a separate group, assigning them to the Pre-Paleozoic. Different aspects of geology of the Western Cis-Onega as a whole and inner structure of red quartzite-sandstones therein in particular were studied by A.A. Inostrantsev, K.K Focht, V. Ramsey, V. Vaal, S.A. Yakovlev, P.A. Borisov, J.J. Sererholm, and other famous scientists of that time. V. Ramsey, by analogy with the sedimentary formations of Björnberg, Finland, was the first to assign the red sandstone unit of the Western Cis-Onega to the Jotnian series. V.M. Timofeev [Timofeev, 1935] combined the Shokha and Kamenny Bor sandstone deposits into a single Jotnian Group of the Upper Proterozoic, having divided it into the Kamenny Bor (lower) and Shoksha (upper) Formations. The reconstructions of sedimentation environment and Jotnian rock transformation are considered in the publications of K.O. Krats [Krats, 1955], L.P. Galdobina [Galdobina, 1958], D.I. Garbar [Vigdorchik et al., 1968; Garbar, 1971], I.M. Simanovich [Simanovich, 1966, 1978], and M.G. Leonov [Leonov et al., 1995].

The Shoksha Formation cross-section has a three-membered structure [Sokolov, 1987]. The basement rock of the lower Shoksha sub-formation comprises oligomictic conglomerate lenses whose pebble is mainly represented by quartz and chalcedony and more rarely by sandstones and aleurolites of the Petrozavodsk Formation. The lower part of the sub-formation cross-section displays a coarse rhythmic pattern. Some rhythms are 1.5 to 4.0 m in thickness and composed of coarse- and middle-grained quartzite-sandstones of red, pink or crimson color, often with the alluvial or delta-type trough cross-bedding. The upper rhythms comprise thin interlayers with fine-grained quartzite-sandstones, aleurolites and argillites, with their bedding surface largely marked by wave and flow ripples, raindrops and flowing water, underwater landslide textures, and mud cracks. The upper part of the sub-formation is composed of fine-grained quartzite-sandstones, aleurolites, and dark-cherry schists. The lower sub-formation may reach 300 m in thickness.

The basement rock of the middle Shoksha sub-formation is represented by alternating oligomictic boulder conglomerate and sandstone lenses. Higher in the succession there lie the middle- and fine-grained quartzite-sandstones of pink and pale violet color, aleurolites and argillites. The sub-formation cross-section displays generally a rhythmic pattern – the rhythms are 1.5–2.0 m thick in the lower part, decreasing in thickness with an increase in the proportion of fine-grained varieties higher in the succession. The middle sub-formation is 300–700 m thick.

Most of the upper Shoksha sub-formation is composed of middle- and coarse-grained feldspar-quartz sandstones, with its thickness estimated at 200 m.

The total thickness of the Shoksha Formation is somewhat more than 1000 m.

The rocks of the Shoksha Formation in the region of the same-name deposit erosively overlie the sandstones of the Petrozavodsk Formation. Lying with prominent stratigraphic and angular unconformities in the weathering crust, the Shoksha basement deposits are overlain by the Vendian sediments.

5. THE STRUCTURE OF THE SHOKHA DEPOSIT AND KL-555 SAMPLING SITE

The Shoksha deposit of facing and building stones is situated on the southwestern coast of Lake Onega in 45 km to the southeast of Petrozavodsk city (Fig. 4). The deposit area consists of sandstones and quartzite-sandstones of the Petrozavodsk and Shoksha Formations (Fig. 5). It also comprises the stratotype of the lower part of the Shoksha Formation cross-section [Galdobina, 1958; Sokolov, 1987].

The deposit layers gently dip southward at an average angle of 5 to 15 degrees. They are complicated by the NNE-striking faults and gentle folds (Fig. 5), and small (0.2–5.0 m) intralayer asymmetric folds with different orientations (Fig. 6, a, b).

The deposits of the Shoksha Formation erosively overlie gray and brownish-gray sandstones of the Petrozavodsk formation and consist of succession of layers of monomictic quartzite-sandstones and sandstones (from bottom to top).

1) Pale lilac quartzite-sandstones with a small-pebble-conglomerate interbed in the basement and ripple marks on the bedding surfaces (more than 5 m);

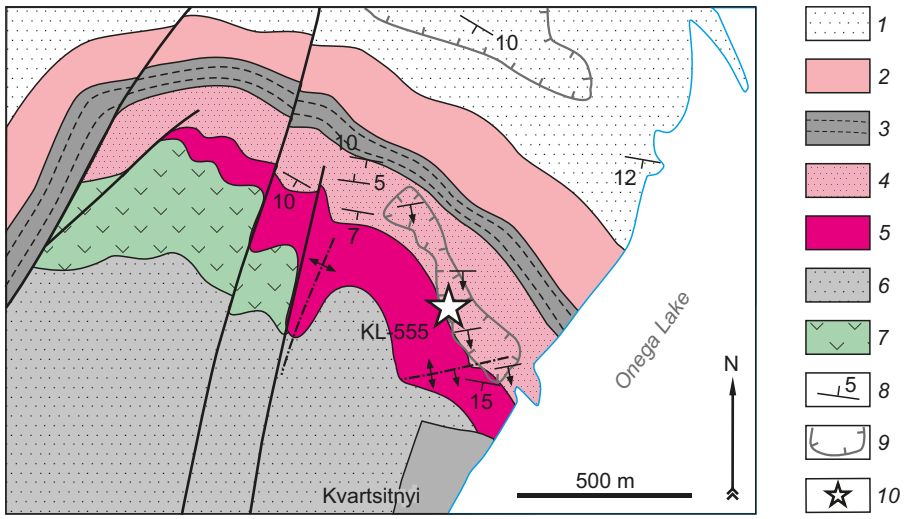

Fig. 5. The scheme of the geological structure of the Shoksha quartzite-sandstone deposit.
1 – arkose sandstones of the Petrozavodsk Formation; *2–6* – sediments of the Shoksha Formation: *2* – lilac quartzite-sandstones, *3* – intercalation of siltstones, shales and sandstones, *4* – red quartzite-sandstones, *5* – crimson quartzite-sandstones, *6* – gray-pink sandstones; *7* – basalts; *8* – dip and strike of rock layers; *9* – contours of the quarries; *10* – KL-555 sampling site.

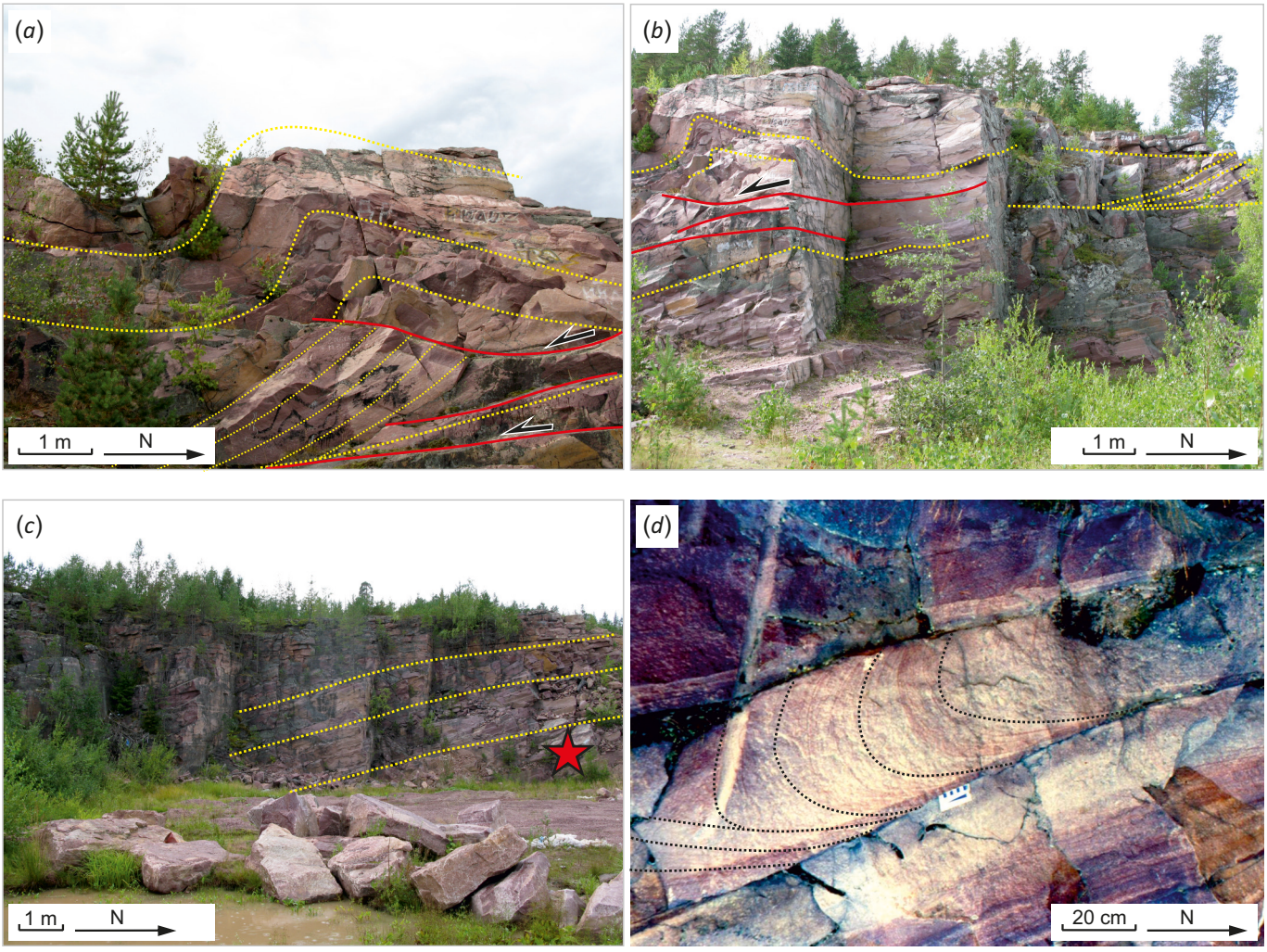

Fig. 6. The southern quarry of the Shoksha deposit of quartzite sandstones.
(*a*) – oblique layering and asymmetric fold of underwater landslide in quartzite-sandstones; (*b*) – sublayer detachments in quartzite-sandstones and associated drag folds; (*c*) – site of KL-555 sampling (asterisk) of quartzite-sandstones in the south-western wall of the quarry; (*d*) – small folds of underwater landslide, complicating oblique stratification in quartzite-sandstones.

2) A member of alternating red and greenish aleurolites, clay-mica schists and fine-grained sandstones (5 m);

3) Cross-bedded red fine-grained quartzite-sandstones with wave and flow ripple marks (14 m);

4) Large cross-bedded sets of crimson fine-grained quartzite-sandstones which are the most industrially important (17 m);

5) Cross-bedded grayish-pink quartz sandstones with gravelite basement layers (40 m).

Sample KL-555 was taken from the upper cross-section of red quartzitic sandstone layer 3 (see below for details) to obtain dZr grains (see Fig. 5; Fig. 6, c). Layer 3 – KL-555 sampling site – is complicated by con-sedimentary diagenetic structures and textures. There occur large and medium-sized cross-bedded sets of fluvial or deltaic origin with predominantly south-southeast-tilted strata (160–170°) (Fig. 6, a, b). There are also some isolated sets of trough cross-bedding. The upper part of layer 3 in the studied artificial exposure is complicated by an intralayer con-sedimentary asymmetric fold with amplitude of about 3m (Fig. 6, a). The fold is characterized by the southern vergency consistent with cross-bed tilting and, therefore, with tilting angle of the sedimentary basin paleoslope. These features imply that the fold was formed due to underwater-sliding layers and controlled by sublayer detachment in the structure basement (Fig. 6, a). Smaller landslide folds complicating cross-bedded sets in layer 3 are found throughout the section (Fig. 6, d).

The overlapped structural and material transformations of quartzite-sandstones in layer 3 are represented by brittle and brittle-plastic deformations. They manifest themselves in the form of slip joints and slickensides, metagenetic recrystallization and regeneration of fragmented quartz grains, and quartzitic sandstone secondary striation. During metagenesis and early stages of metamorphism, the Shokha sandstones underwent uneven recrystallization and compaction, with iron ochres transformed into hematite plates which have become a source of different colors of the rocks. Metagenetic transformations of the Shoksha sandstones are considered in detail in specialized publications [Leonov et al., 1995; Simanovich, 1966, 1978].

One of the reasons for secondary transformations of the Shoksha quartzite-sandstones might be fluid-thermal effect caused by the flows of basalts and gabbrodolerite sills deposited at different levels of the Shoksha Formation cross-section. For example, layers 3 and 4 in the western part of the Shoksha deposit are separated by the basaltic cover that might have exerted a thermal effect on the underlying quartzite-sandstones (layers 1–3), which were later erosively overlain by somewhat less epigenetically modified sandstones of layer 4.

6. THE RESULTS OF STUDY OF DETRITAL ZIRCON GRAINS OBTAINED FROM THE SHOKSHA FORMATION QUARTZITE-SANDSTONES (SAMPLE KL-555)

With the aim of obtaining dZr grains and their further U-Pb isotopic dating, there was taken the KL-555 sample from the quartzite-sandstones in the lower part of the Shoksha Formation (upper part of layer 3 of the Shokha deposit described above). The sample was taken in the southwestern wall of the southern quarry of the Shokha deposit, 300 m north of Quaternary settlement margin, at coordinates 61°30'12.01 N; 35°02'57.40 E (see Fig. 5; Fig. 6, c).

6.1. Microscopic study of quartzitic sandstone sample KL-555

Microscopic study of quartzitic sandstone sample KL-555 showed that quartzite-sandstones are mainly composed of quartz (Fig. 7). The rock sample is muted pink, pale beige in thin sections. The fragments consist of 95 % quartz, with some of them dominated by microquartzites. The accessory minerals are zircon, apatite, magnetite, and hematite. The quartz grains undergo significant regeneration and partial recrystallization. There occur both oval and angular grains, most of which are irregularly shaped, sometimes elongated.

The rock structure is irregularly-grained psammitic-blastic from fine- to medium-grained (Fig. 7, a, b). The texture is striated due to alternating stripes with larger (0.2–0.6 mm) and smaller (0.05–0.1 mm) grains. There are two types of cement: quartz regeneration (3–5 %) and porous quartz-chlorite-mica (7–15 %) (Fig. 7, c, d). In some pores there are mica rosettes. There also occur thin crustified mica rims. Noteworthy are regeneration quartz rims with clearly defined crystallographic contours and abundant blastic displacement structures (grain boundary migrations).

There occur incorporated, less frequently sutured quartz grain contacts, blastic displacement structures, and regeneration rims. Quartz grains show undulatory, block and mosaic extinction, Boehm stripes, and sometimes splintery fractures in grains (Fig. 7, e, f).

6.2. Study methods for detrital zircon grains from sample KL-555

Sample preparation, ways to get zircon grains, analytical preparation, preliminary preparation of zircon grains for isotopic analysis, processing of primary analytical results, age-date selection, ways to analyze zircon-grain dating results and other procedures were performed in accordance with study methods described in [Romanyuk et al., 2018]. Sample KL-555 (initial weight ~1.5 kg) was grinded without a grinder in a cast-iron mortar to size class –0.25 mm and passed through a one-use kapron sieve fixed to the steel frame. The grinded material was washed out successively by pipe-run water, air-dried, separated using heavy liquid HPS-W (~2.95 g/cm^3), and underwent magnetic separation. The dZr grains were selected randomly from non-magnetic heavy fraction by the manual microscopic method. These grains were implanted into an epoxy disk and polished manually to about half the size of typical grains. The polished dZr-grain parts without fractures, inclusions and other imperfections, and no less than 40 microns in diameter were selected for laser ablation U-Pb zircon dating.

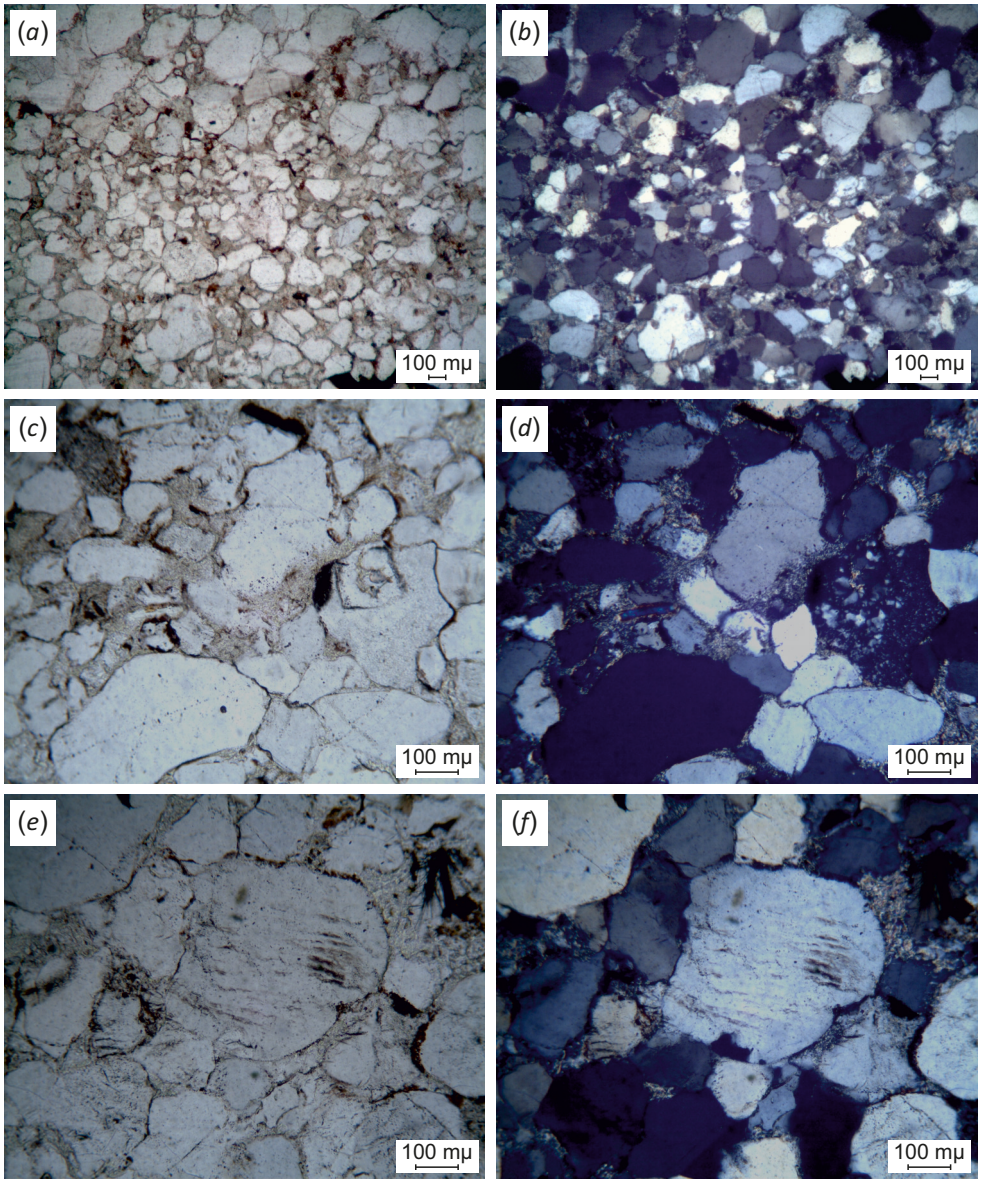

Fig. 7. Micrographs of quartz sandstone sections of the KL-555 sample. On the left there are parallel nichols, on the right – crossed nichols. See text for explanation.

The study of U-Pb isotopic system of dZr grains from sample KL-555 was conducted at the Shared Research Facilities of the GIN RAS with ESL NWR213 Laser Ablation System combined with ELEMENT2 (Thermo Scientific Inc.) high resolution magnetic sector mass spectrometer. The analytical research method and operational characteristics of the device are described in [Nikishin et al., 2020]. The U-Pb isotope data for the selected parts of dZr grains were primarily processed using GLITTER software [Griffin et al., 2008]; the correction for non-radiogenic lead were calculated based on the procedure described in [Andersen, 2002] and realized as part of ComPbCorr program [Andersen, 2008]. Histograms and probability density curves (PDC) are drawn using free-access ISOPLOT program [Ludwig, 2012].

The analytical measurements were calibrated based on external zircon standard GJ-1 [Jackson et al., 2004; Elhlou et al., 2006]. Analytical quality control was carried out by measuring unknown samples and reference standards of 91500 [Wienedbeck et al., 1995, 2004] and Plesovice [Sláma et al., 2008] zircons in combination with the weighted mean $^{206}Pb/^{238}U$ (2σ) ages of 1063.5±0.4 and 337.2±0.1 Ma, respectively [Horstwood et al., 2016]. For these reference standards there were obtained the weighted mean (2σ) ages of 1067.8±7.0 (n=8) and 332.6±5.2 (n=7) Ma, respectively, which are consistent within the error with the above-presented weighted mean $^{206}Pb/^{238}U$ (2σ) ages obtained by the CA-ID-TIMS method [Horstwood et al., 2016].

6.3. Results of U-Pb isotope analysis of zircon grains

There were analyzed 79 dZr grains from sample KL-555 (App. 1, Table 1.2). GLITTER software makes it possible to see the time scan (we call it an analytical signal) of the recorded number of ions ^{206}Pb, ^{207}Pb, ^{208}Pb, ^{232}Th and

^{238}U with a laser beam penetration into the zircon grain studied, i.e., the evaporation of substance from its deeper and deeper parts. Different parts of an analytical signal correspond to different zircon grain parts. Most of the analytical signals recorded are short highly variable records. Some of them yielded age estimates only for their half or a third. In case when the age estimation involved the middle or the beginning of an analytical signal, this part of the record was interpreted as core analysis ("core"). But in case when there was used the final (marginal) part of an analytical signal record, it was interpreted as an analysis of the grain margin ("rim"). However, some records of good duration and quality (the degree of discordance – both of the first two percent units, D1 and D2) showed the age estimates in the interval from 1.91 to 1.95 Ma. The results of analyses are displayed in a concordia diagram (Fig. 8, a).

A larger number of the analytical results is characterized by high degree of discordance of the date values calculated therefrom – inconsistency in the age dates calculated from different isotope pairs. To characterize the degree of discordance, there were used values D1 и D2 calculated by formulas (1) and (2):

$$D1=100\ \%\cdot[\text{age}\ (^{207}Pb/^{235}U)\ /\ \text{age}\ (^{206}Pb/^{238}U)-1], \quad (1)$$

$$D2=100\ \%\cdot[\text{age}\ (^{207}Pb/^{206}Pb)\ /\ \text{age}\ (^{206}Pb/^{238}U)-1]. \quad (2)$$

34 analyses yielded – 1.2 %<D1 and D2<10 %, and common lead age correction by <60 Ma which were used for drawing a histogram and a PDC. All these dZr grain ages obtained are older than 1 Ga so that the ages were only estimated from $^{207}Pb/^{206}Pb$ ratios (Fig. 9).

The youngest ages are 1899±12 Ma (D1=2.9 %, D2= 6.3 %), 1904±11 Ma (D1=0.0 %, D2=0.05 %), and 1913 ±11 Ma (D1=–0.6%, D2=–1.2%); the oldest ages – 2777 ±7 Ma (D1=2.0 %, D2=3.4 %) and 2805±11 Ma (D1=0.4 %, D2=0.7 %). The major peaks in the PDC visualizing the age dates, based on more than 5 measurements, correspond to 1920 and 2006 Ma; the 3-measurement-based secondary peak – to 2078 Ma.

The U-Pb ages obtained are subdivided into two groups: ages within the middle and late parts of the Early Proterozoic and the Late Archean ages. The Early Proterozoic age dates comprise a dense, dominant set with the age intervals 1.90–1.96 Ga (18 dates) and 2.05–2.08 Ga (3 dates). The ages of six Late Archean single zircon grains fall within the interval 2.5–2.8 Ga. Therefore, the analysis of results of U-Pb isotopic dating for dZr grains from the Shoksha quartzite-sandstones (sample KL-555) suggests that the Shoksha Formation sandstones were formed due to the accumulation of detritus from the crystalline complexes whose age corresponds primarily to the middle and late parts of the Early Proterozoic and to the Late Archean.

A large (more than a half) number of strongly discordant age dates obtained testifies to the fact that the dZr grains from the Shoksha quartzite-sandstones experienced thermal-metamorphic and/or hydrothermal-metasomatic effect which was probably multiple. This effect disrupted to a varying degree (sometimes severely) the U-Pb system of the grains dated. The analysis which yielded the age dates for the "core" or "rim" are plotted in the concordia diagram (see Fig. 8, a) in the form of an elongated area which allows drawing a discordia line or discordia line series. This discordia has a good fit to many points

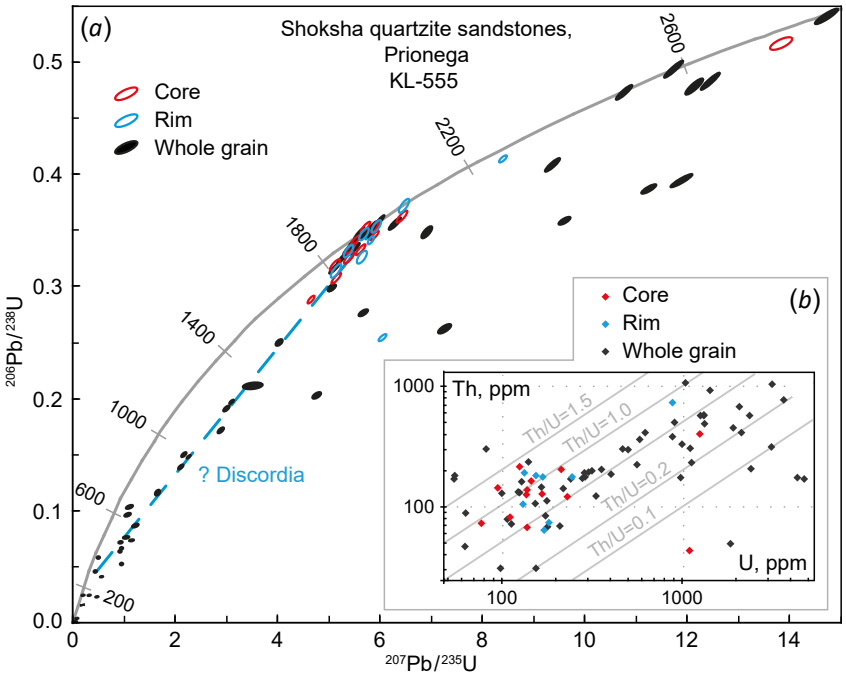

Fig. 8. Results of the study of detrital zircons from sample KL-555.
(*a*) – diagram with concordia for U-Pb dating. The blue dashed line is an inferred possible discordia line; (*b*) – "Th versus U" diagram (logarithmic scale).

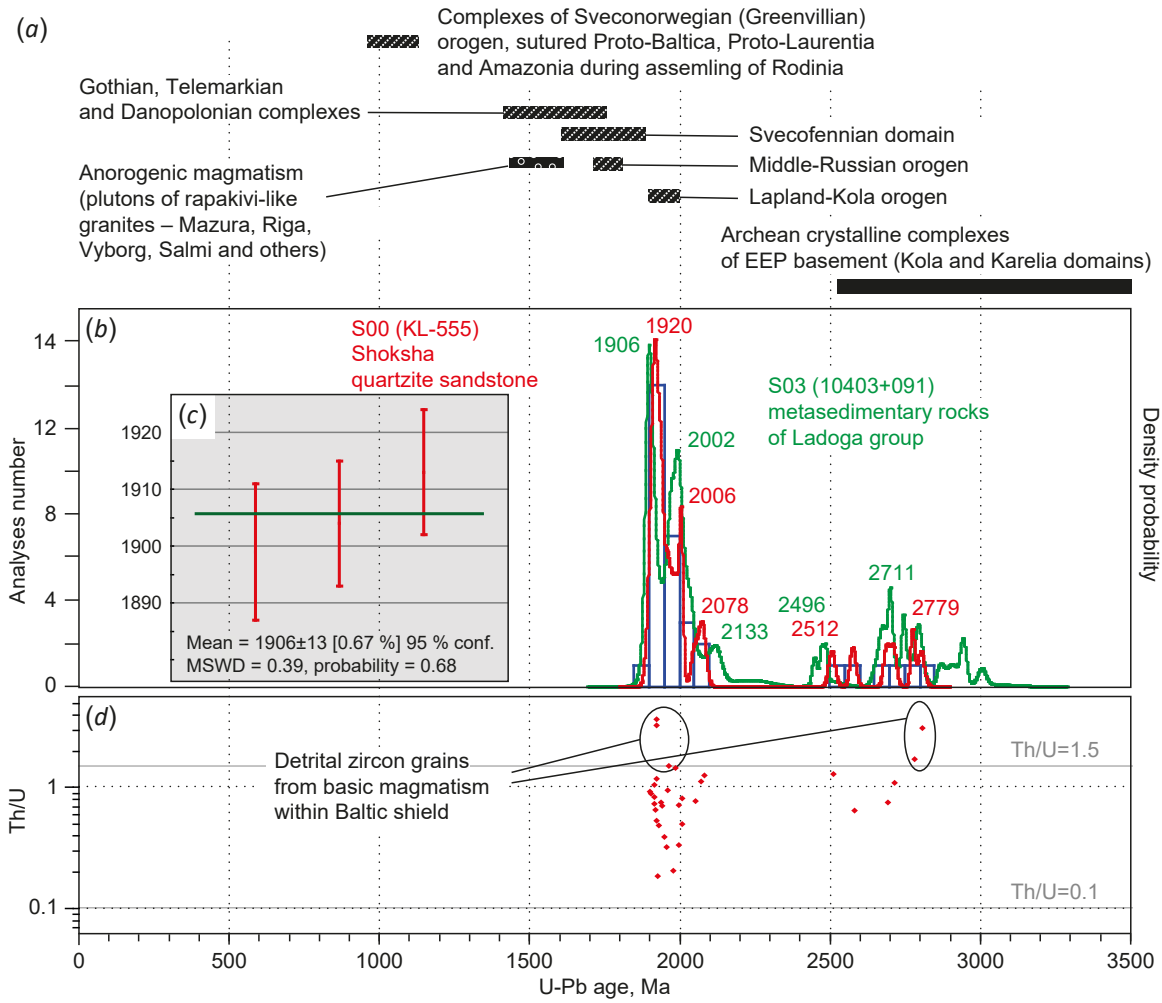

Fig. 9. A summary of the ages of some crystalline complexes of the northern part of the EEP, which could be the potential primary sources of detrital zircons (*a*). Histogram and PDC (density probability plot, red line) illustrating the distribution of U-Pb isotopic ages of dZr grains from the KG-555 sample (*b*). The green line is PDC for the metapelites of the Ladoga Group [Sharov, 2020]. Weighted average value obtained from three youngest ages (*c*). Diagram "Th/U vs U-Pb age" for the studied dZr grains, for which conditional age estimates were obtained (*d*).

corresponding to discordant analyses of the whole grain. The accuracy of estimation of the lower intersection of the concordia and discordia lines remains low. These are only the overlapped formations that can be confidently assigned to the Phanerozoic.

6.4. Interpretation of Th/U values in dated detrital zircon grains from sample KL-555

Thorium/uranium ratios (Th/U) in zircon from magmatic rocks (i.e. in magmatogenic zircon) vary from 0.1 to 1.0 [Kirkland et al., 2015; Rubatto, 2017]. Low Th/U values are considered to be statistical characteristic of metamorphogenic zircon grains. An inferred threshold value of Th/U providing for separation between magmatogenic and metamorphogenic zircon, presented in published papers, is therewith different: 0.5 in [Kirkland et al., 2015], 0.2 in [Hoskin, Schaltegger, 2003] and 0.1 in [Teipel et al., 2004]. It is most likely that the Th/U values of 0.1 to 0.5 are also be often found in both magmatic and metamorphic zircon.

Along with other characteristics, high thorium-to-uranium ratios (Th/U>1.5) are inherent to statistics for melanocratic (mafic) magmatic zircon [Kaczmarek et al., 2008; Linnemann et al., 2011]. It is also worthy of note that high Th/U in zircon is sometimes typical of the rocks formed in high-temperature and lower-to-moderate-pressure metamorphic environment [Wanless et al., 2011]. The zircon crystallized in low-temperature granites is characterized by high U and low Th contents. It is usually described in terms of low Th/U in low-temperature zircon [Harrison et al., 2007].

The analysis made on 79 dZr grains from sample KL-555 yielded Th content varied from 30.6 to 1073.1 ppm and U content varied from 54.5 to 4765 ppm, with Th/U values varied from 0.03 to 3.72 (see Fig. 8, b). Five grains yielded very low thorium-to-uranium ratio (Th/U<0.1). These dZr grains might have originated primarily from (ultra) high-pressure complexes (eclogites) or, for example, such "exotic" complexes as ultra-low temperature granitoids. However, the age estimates for these grains appeared to be

discordant, which does not provide for the possibility of their reliable and meaningful interpretation.

A considerable part of the analyses (14) yielded the Th/U ratios higher than 1.0, among which five are even higher than 1.5. Three analyses yielded uniquely high Th/U ratios: № 54 – 1922 Ma Th/U=3.72; № 68 – 1920 Ma Th/U= =3.30; № 74 – 2805 Ma Th/U=3.12. This implies that among primary sources of dZr grains for which such Th/U values were obtained there might have been the complexes with frequent occurrence of mafic rocks (for example, basalts and gabbroids) and/or the rocks undergone high-temperature metamorphism (for example, granulites). These are most likely magmatic zircons from the rocks of the Suisar complex.

Nevertheless, most of the analyses yielded Th/U ratio range of 0.1 to 1.0. Such thorium-to-uranium ratio values are considered to be statistical characteristics of magmatogenic zircon from siliceous and intermediate rocks. The dZr grains with such Th/U ratios most likely originated from usual granitoids with normal or low levels of silica acidity or from their volcanic equivalents.

7. ON THE AGE OF QUARTZITE SANDSTONES OF THE SHOKSHA FORMATION AND THEIR REAL TRANSFORMATION TIME

The Shoksha Formation (Shoksha horizon) comprising the upper section of the Vepsian sub-horizon in the upper Lower Proterozoic rocks of the Baltic Shield. The lower age limit of the Vepsian is confined to the Lyudikovian magmatic and volcanogenic-sedimentary rocks (2100–1920 Ma), on which it lies unconformably, and the upper age limit is confined to the gabbrodolerites of the Ropruchei complex, isotopically dated at 1770–1750 Ma [Bibikova et al., 1990; Lubnina et al., 2012], which form sills cutting through the Shokha Formation. The Lake Onega's sediments of Kalevian (1920–1800 Ma), lying stratigraphically between the Lyudikovian and Vepsian, remain undated.

The weighted average of the three youngest dates recorded is 1906±13 Ma (Fig. 9, c) and can be considered the lower age limit of the Shoksha Formation rock. This result is generally consistent with the modern ideas of assigning the Shoksha Formation to the uppermost Lower Proterozoic [Negrutsa, 2011; Kulikov et al., 2017a, 2017b; and others].

The sedimentary breccia and conglomerate interlayers in the basement of the Shoksha Formation (upper Vepsian sub-horizon) comprise different-sized fragments of the Jatulian quartzites, Lyudikovian shungite-containing rocks and volcanics, and granitoids, granite-gneisses and other rocks typical of the inner structure of the Archean complexes in the KM basement. Similar fragments are also found in the conglomerate and sedimentary breccia horizons in the Petrozavodsk Formation cross-section (lower part of the Vepsian sub-horizon). This implies that the Shoksha Formation and its underlying Petrozavodsk Formation were formed after the Svecofennian deformations or against the background of the final episodes of folding of this age. Considering that the culmination in the Svecofennian folded strata occurred in the interval 1.9–1.87 Ga [Morozov, 2010; Systra, 1991; Korsman et al., 1999], the Shoksha Formation occurrence time cannot be too distant from the age boundary of 1.87 Ga.

A significant part of the results of isotopic analyses made on dZr grains from red quartzite-sandstones of the Shoksha Formation yielded highly discordant dates. This can imply that the studied dZr grains from the Shoksha Formation were under thermal and/or hydrothermal metasomatic effect, presumably repeated, which disturbed their isotopic systems. The features of distribution of discordant analytical points on the concordia diagram (see Fig. 8, a) suggest that the rocks in cross-sectional area of the Shoksha Formation from which sample KL-555 had been taken experienced this effect in the Phanerozoic. The sampled quartzite-sandstones only bear evidence of initial low-temperature stages of metamorphic changes. This eliminates the possibility for in situ formation of metamorphic zircon grains.

The assumption that discordant dZr grains (in accordance with some isotope ratios assigned to the Riphean and/or Phanerozoic) fell within these Shoksha quartzite-sandstones already altered, i.e. recycled from older rocks, is inconsistent with the geological situation and age boundaries of the Shoksha quartzitic sandstone formation. However, we cannot exclude the possibility of overlapping transformations for dZr grains and, therefore, the occurrence of zircon grains (or their separate parts – marginal zones) therein, with their U-Th-Pb system disturbed due to the radiogenic lead loss or emergence of newly formed hydrothermal-metasomatic zones with an unbalanced U-Th-Pb isotopic system.

It has been earlier shown that the Lower Proterozoic rocks of Zaonega and Suisar Formations in Cis-Onega [Glushanin et al., 2011] contain the discordant zircon grains whose age dates, from some isotopic ratios, correspond to the Riphean and/or Phanerozoic, similar to how it has been determined for dZr grains obtained from the quartzite-sandstones of the Shoksha Formation (sample KL-555). This shows at large-scale hydrothermal transformations of the rocks in the Onega synclinorium. Similarly overlapping transformations of dZr grains, obviously related to a deep-seated fluid rush to the surface, are found in the Riphean rocks composing the rift system of the White Sea [Kuznetsov et al., 2021].

Therefore, the formation time of the Shoksha quartzite-sandstones is constrained to an interval of 1906±13 (weighted average ages of the three youngest dZr grains from these quartzite-sandstones) to 1770–1750 Ma (isotopic age of basites which compose the Ropruchei sill cutting through the Shoksha quartzites). This is generally in good agreement with today's concept of the age of the Shoksha Formation as the upper stratigraphic element of the Vepsian sub-horizon of the cumulative stratigraphic scale of the Lower Precambrian eastern Baltic Shield [Negrutsa, 2011; Kulikov et al., 2017a, 2017b; and others]. A rather long (almost 150 Ma) time interval, in which there falls the occurrence time of the Shoksha Formation, will evidently

be reduced in the future. The lower age limit can be refined and rejuvenated, for example, due to obtaining dZr grains younger than 1899 Ma (the age estimate of the youngest dZr grain with an acceptable concordance in sample KL-555). However, the isotopic system is highly disturbed in younger isotopic dZr grains obtained based on some isotopic ratios from sample KL-555. This does not allow using these dates to constrain the lower age limit of the Shoksha Formation but shows that the Shoksha quartzite-sandstones underwent a significant transformation in the Phanerozoic.

8. POSSIBLE ORIGINS OF DETRITAL ZIRCON GRAINS FROM THE SHOKSHA QUARTZITE-SANDSTONES

The analysis of dates for dZr grains from the Shoksha quartzite-sandstones (sample KL-555) shows that these rocks were formed due to accumulation of clastic material brought by sediment flows which transported detritus originated from mostly Early Proterozoic, rarely Late Archean crystalline complexes (Fig. 9, b). The predominant groups of dZr grains with age intervals 2.1–1.98 Ga (6 dates), 2.05–2.08 Ga (3 dates) and 1.96–1.90 Ga (18 dates) most likely originated from the crystalline complexes – magmatic rocks which contributed to the Lyudikovian sediments – Zaonega and Suisar Formations (2100–1920 Ma) of the northern Onega synclinorium (see Fig. 4). The major peak in the frequency (~1.92 Ga) of the dates for dZr grains from the Shoksha quartzite-sandstones implies the existence of local (close to the sedimentation area) detrital source whose contribution was larger than that of the other sources (Fig. 9, b). This isotopic age corresponds to the upper age limit of the Lyudikovian sub-horizon and is close to the age of dolerites intersecting the rocks of the Zaonega horizon – 1919±18 Ma (SIMS, n=12, MSWD=0.18, Th/U from 0.2 to 0.56) [Priyatkina et al., 2014]. The dolerites dated at 1956±5 Ma (SIMS; n=9; MSWD=0.18, Th/U from 1.81 to 3.72) [Stepanova et al., 2014a] and the Zaonega complex volcanites dated at 1982±4.5 and 1961±5.1 Ma (ID-TIMS) [Martin et al., 2015] might be a significant contribution to the accumulation of dZr grains. Among six dZr grains (2.1–1.98 Ma) from sample KL-555, there can be some that were derived by erosion of the Konchezero sill dated at 1975–1980 Ma, Th/U from 1.75 to 4.63 [Puchtel et al., 1992, 1998].

The conclusion that the Lyudikovian magmatites could be a source of most of the dZr grains from sample KL-555 is confirmed by high thorium-to-uranium ratios exceeding 1.0 and even 1.5 for considerable part of the dates (14). Such values are typical of zircon from mafic rocks – basaltoids and gabbroids and/or high-temperature granulites. The last (granulites) are less probable because there were no such rocks found in the KM to the north and northwest of the sampling site. However, we cannot exclude a distant dZr grain provenance in granulites. This can be complexes of the Belomorian-Lapland, Svecofennian or South Finland-Ladoga belts (more than 300 km transportation distance) (see Fig. 2).

The six single Late Archean dZr grains from sample KL-555 have an age interval spanning from 2.8 to 2.5 Ga. These dates are in good agreement with those obtained for granitoid rocks of the tonalitic series penetrated by the Onega parametric borehole in the basement of the same-name synclinorium [Glushanin et al., 2011]. The magmatic stage of granite formation is estimated at ~ 2820±13 Ma. The younger age estimates of these granites (2711±17 and 2739±19 Ma) can determine the stages of their secondary (metamorphic) transformation. A number of even more younger ages – 2547±26, 2525±52, 2453±13 and 2406 ±16 Ma – reflect at least two-stage transformation of rocks at the boundaries 2520–2560 and 2400–2450 Ma. However, the Archean basement rocks penetrated by the Onega parametric borehole are not exposed so that their occurrences as provenance areas raise questions. This can be interpreted in three ways.

1. The Late Archean dZr grains from sample KL-555 originated from granitoids of the basement of the Onega synclinoriunm, which were squeezed to the surface during deformation evolution of this structure and involved in the formation of the cores of narrow diapiric anticlines.

The granitoid protrusions of this type can still be found at the north of the Onega synclinorium. Apogranite blastomylonites participating in the structure of these protrusions were dated by the Rb-Sr method on rock in a wide age range (1830±10 Ma, 1670±60 Ma, 1270±50 Ma), which testifies to a long period of secondary transformation in the Archean rocks [Kolodyazhny et al., 2000].

2. The Late Archean dZr grains from sample KL-555 originated from granitoids widespread along the western margin of the KM Vodlozero domain are related to the stage of rheomorphism of granite-gneiss domes [Miller, 1988]. Thus, within the Vodlozero-Segozero greenstone belt, there were found granodiorite massifs of the sanukitoid series with ages of 2743±8 Ma [Bibikova et al., 2005a] and 2745 ±5 Ma [Ovchinnikova et al., 1994].

3. The Late Archean dZr from sample KL-555 came from sediment-distant landsources in the central and western provinces of the KM whose structure is characterized by widespread Middle- and Late Archean granite-greenstone associations [Lobach-Zhuchenko et al., 2000; Hölttä et al., 2014]. The occurrence time of reginal metamorphism of the Late Archean rocks developed therein is estimated at 2720 and 2700 Ma [Kulikov et al., 2017a, 2017b; Shcherbak et al., 1986]. Approximately the same age was obtained for sanukitoids comprising vast fields in the western and central sub-provinces of Karelia [Samsonov et al., 2001; Bibikova et al., 2005b]. Late Archean (Lopian) metamorphism was related to the formation of thermal granite-gneiss domes whose borders are isolated zonal metamorphic complexes of greenstone belts [Miller, 1988].

It is necessary to take into account the fact that among dZr grains from sample KL-555 there are no Early Archean tonalitic rock materials dated at 3210±12 Ma [Levchenkov et al., 1989], 3500 Ma [Sergeev, Berezhnaya, 1985; Sergeev et al., 1990, 2007], 3822±48 Ma [Smolkin, Sharkov, 2009], and 3871±39 – 3837±42 Ma [Kozhevnikov, Skublov, 2010;

Kozhevnikov et al., 2006, 2010]. These rocks occur widely on the northeastern side of the Onega synclinorium.

The oldest dZr grains, older than 3.6 Ga, were found in red metagravellites of the Luchlompol Formation of the North Pechenga Zone (S09, Fig. 10) [Smolkin et al., 2020] compared with the Upper Jatulian of the KM. Besides, 3.6 Ga and even older dZr grains were found in the KM Jatulian rock units. Rather old dZr grains up to 3837±42 and 3871 ±38 Ma were earlier found respectively in the Jatulian quartzite-sandstones of the Volomskaya syncline and in sand-matrix Jatulian conglomerates of the northwestern centroclinal zone of the Onega synclinorium (S04, Fig. 10) [Kozhevnikov et al., 2010]. This implies that in the eastern Baltic Shield and adjacent areas could be the occurrence of these old crystalline rocks yielding detritus transported into the Shoksha sedimentary basin or at least Early Archean or Hadean dZr grains recycled from the Jatulian rocks. However, such old dZr grains were not found in the Shokha quartzite-sandstones. What could have isolated the Shoksha sedimentary basin from the eroded materials containing the oldest zircon? Perhaps, the entire vast area including the KM Vodlozero domain was a sediment accumulation area in Vepsian time. However, this is not consistent with the currently dominant views of the development of the South Onega paleobasin in the contours close to its modern boundaries [Glushanin et al., 2011]. A suggestion about a wide development of still poorly known Late Archean granite-gneiss domes within the KM Vodlozero domain seems to yield the conclusion that it is precisely these domes which formed the further eroded uplands. In any case, the source areas on the South Onega basin slopes did the least to transport the dZr grains.

5 dZr grains from sample KL-555 had very low thorium-to-uranium ratios (Th/U<0.1). That probably means that these dZr grains originated primarily from ultra-high-pressure complexes – such as, for example, eclogites. These complexes are found within the Belomorian-Lapland belt near Salma, Kuru-Vaara and Gridino [Slabunov et al., 2019]. The inner structure of all these complexes is complicated due to the Archean and Paleoproterozoic magmatic and structural-metamorphic transformations [Berezin et al., 2012; Dokukina et al., 2014; Mints, Dokukina, 2020; Skublov et al., 2011; Travin, 2015; Slabunov et al., 2019].

The studies of zircons from these complexes showed that the crystals more often have inhomogeneous structure due to domains, cores and rims therein. These eclogite zircon crystals yielded ages of 1.8 to 2.9 Ga, clustering near the boundaries ~1.9, 2.4 and 2.7–2.8 Ga. Though "the eclogite Th/U ratios" are not evidence of the eclogite origin of zircon grains, it can be supposed that it is precisely the eclogites of the Belomorian-Lapland belt which comprised 5 dZr grains from sample KL-555.

Lastly, there should be mentioned almost best-fit PDC of ages of zircon grains from the Shoksha quartzite-sandstones (sample KL-555) and metapelites from the Ladoga Group (S03) [Sharov, 2020] (see Fig. 9, b). This makes it more likely that the Shoksha quartzites were primarily formed through the recycling of the rocks of the Ladoga Group developed along the boundary between the KM and Svecofennian accretionary orogen (transport distance 200–300 km).

9. PALEOGEOGRAPHIC INTERPRETATION

The dates obtained for dZr grains from the Shoksha quartzite-sandstones (sample KL-555) imply that their lower age limit is close to 1.91 Ga (the weighted average of three youngest dZr grains). The upper age limit of the Shoksha Formation corresponds to the age of gabbrodolerites (1.77–1.75 Ga) which compose the Ropruchei sill cutting through the Shoksha quartzite-sandstones [Bibikova et al., 1990; Lubnina et al., 2012]. The time interval between the upper and lower limits accounts for final stages of assembling of the Columbia (Nuna) Supercontinent. One of such stages is the culminated formation of the Lapland-Kola (Belomorian-Lapland) orogen dated at 1.93–1.91 Ga [Nironen, 1997; Daly et al., 2006; Lahtinen, Huhma, 2019] and Middle Russia orogeny – 1.85–1.7 [Samsonov et al., 2016].

If the Shoksha Formation is confined to the upper age limit, i.e. to about 1.75 Ga, then its quartzitic sandstone constituents would have traces of the Middle-Russian orogeny which at that time was the dominant geomorphic event within the EEP. However, no dZr grains with ages corresponding to the formation of the Middle-Russian orogeny were found in the Shoksha quartzite-sandstones.

On the other hand, if the Shoksha Formation takes its origin from the beginning of the above-mentioned time interval, i.e., from about 1.91 Ga or somewhat later time, then its detrital constituent might have been derived from the complexes of the Lapland-Kola (Belomorian-Lapland) or Svecofennian orogens. The Shoksha Formation is largely characterized by highly mature quartz sandstone constituents. This implies distant detrital sources or, more likely, continually rewashing and recycling older sediments – eroded materials redeposited from the complexes of the Lapland-Kola orogeny – contribute to the second and further sedimentation cycles. It should be emphasized that this conclusion is consistent with the dominant age range from 1.9 to 2.0 Ga revealed by dated dZr grains from sample KL-555 (Fig. 10), which also corresponds to the formation time of the island-arc complexes of the Svecofennian accretion belt (2.2–1.9 Ga).

The Vepsian sub-horizon's formations appear to have accumulated in the South Onega sedimentary basin whose relicts compose the same-name trough. North of it there are the areas of the Lower Proterozoic formations participating in the structure of the constituent parts of the North Onega synclinorium (see Figs. 2, 3, 4). By the beginning of the Vepsian accumulation, these formations had already undergone the main stages of the syn-Svecofennian deformations. Core material of their-realated diapiric anticlinal ridges, complicating the structure of the North Onega synclinorium, is truncated by a paleoerosional surface that exhibits highly tectonized formations in the lower and middle parts of the Early Proterozoic KM proto-sediment cover and its Archean basement rocks. In the Vepsian, these narrow anticlinal faults and folds might have represented

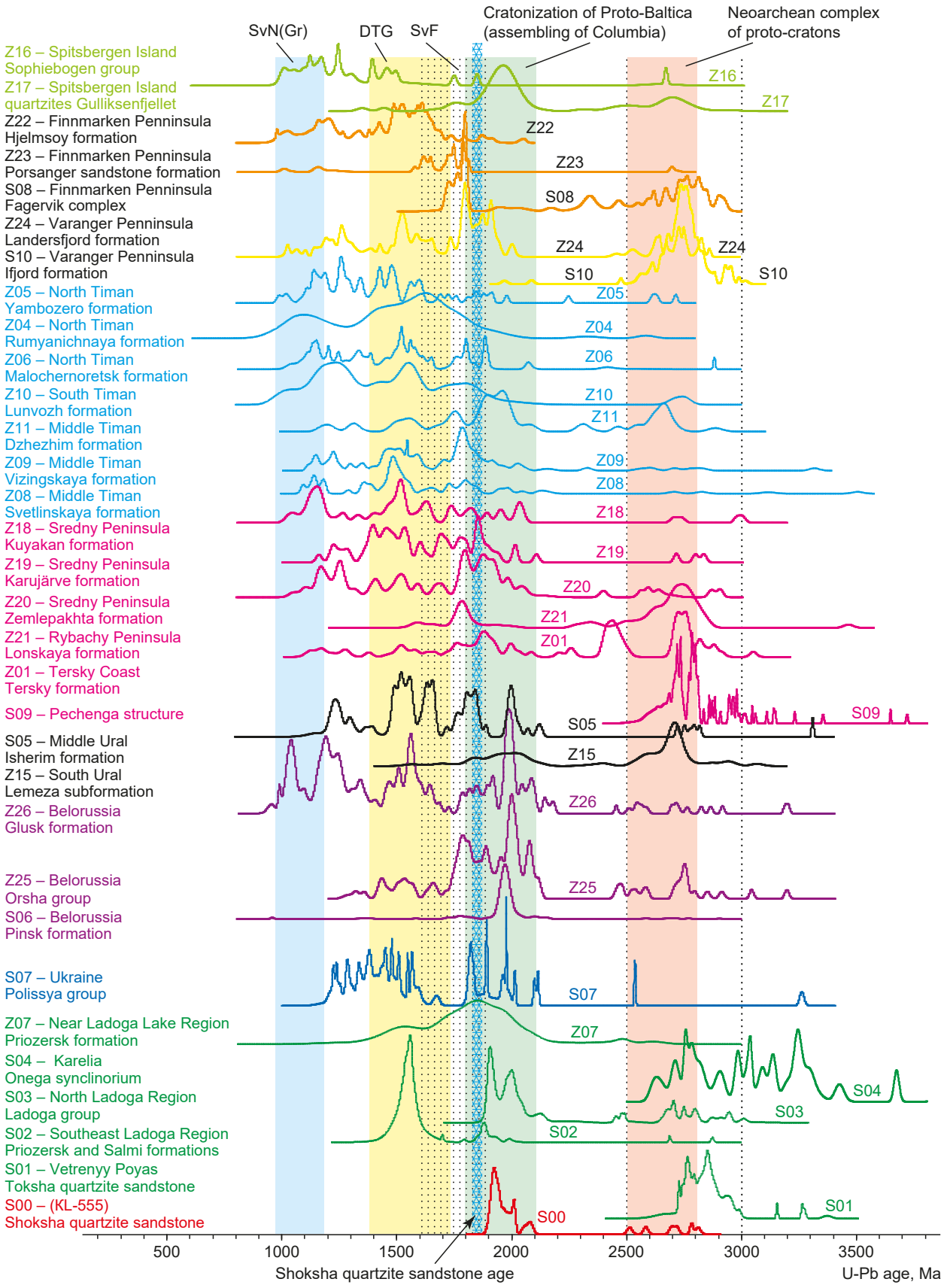

Fig. 10. Summary diagram of the PDC for U-Pb ages of dZr (provenance signals) from the Late Precambrian strata of the EEP and its framing.

Orogens: SvF – Svekofennian, DTG – Dano-Polonian, Telemarkian and Gothian, SvN (Gr) – Sveko-Norwegian (Grenvillian). For data sources, see App. 1, Tables 1.3 and 1.4. The PDC for the Shoksha quartzite-sandstones is shown in red, for the Ladoga region – green, Timan – crimson, Ural – black. The color bands show the age intervals of some tectonic events manifested within the EEP and its framing.

ridge-like upland areas separated by U-shaped valleys of the northwest-to-southeast-flowing rivers which transported the Archean and Early Proterozoic detrital sediments into the South Onega basin. This is evidenced by the Petrozavodsk and Shoksha sedimentary bressias and conglomerates interlayered with different-sized fragments of the Jatulian quartzites, Lyudikovian shungite-containing and volcanic rocks, and Archean granitoids from the anticlinal-ridge cores. From north-northwest to south-southeast transport routes of detritus material are indicated by spatial orientation of the internal pattern of the cross-bedded strata which occur widely in the Shoksha red quartzite-sandstones at the KL-555 sampling site. The cross-beds in these sediments dip generally to the south-southeast. The paleolandslides widespread therein also indicate the south-dipping ancient slopes (see Fig. 6). In a more general context of observations of the cross-bed and ripple-mark orientations, there were also reconstructed the south and south-southeast directions of detrit flow in the South Onega depression [Galdobina, 1958]. These "vector" lithological characteristics suggest that the main detrital-sediment source areas for the Shoksha quartzite-sandstones were located north and northwest of the Shoksha sedimentary basin.

It is also probable that a large amount of the Shoksha-constituent detritus represents the products of recycling of rocks in the Ladoga Group – Kalevian metaturbites of the KM passive margin, – which occur within the Raakhe-Ladoga suture zone along the boundary of the Karelides and Svecofennides (see Fig. 2). This is confirmed by the fact that the age pattern for dZr grains from rocks in the Ladoga Group is visually very similar to the age pattern for dZr grains from the Shoksha quartzite-sandstones (sample KL-555) (Fig. 10). This similarity is supported by a high coefficient p=0.27 of the Kolmogorov – Smirnov test (App. 1, Table 1.5).

The available data suggest a hypothetical reconstruction of the Vepsian branched stream (river network) transporting the detrital material from the north and northwest to the south and southeast (Fig. 11). One of the secondary tributaries might have started in the middle Lapland-Kola (Belomorian-Lapland) orogenic belt (Kandalaksha Gulf of the White Sea), with the source area consisted of

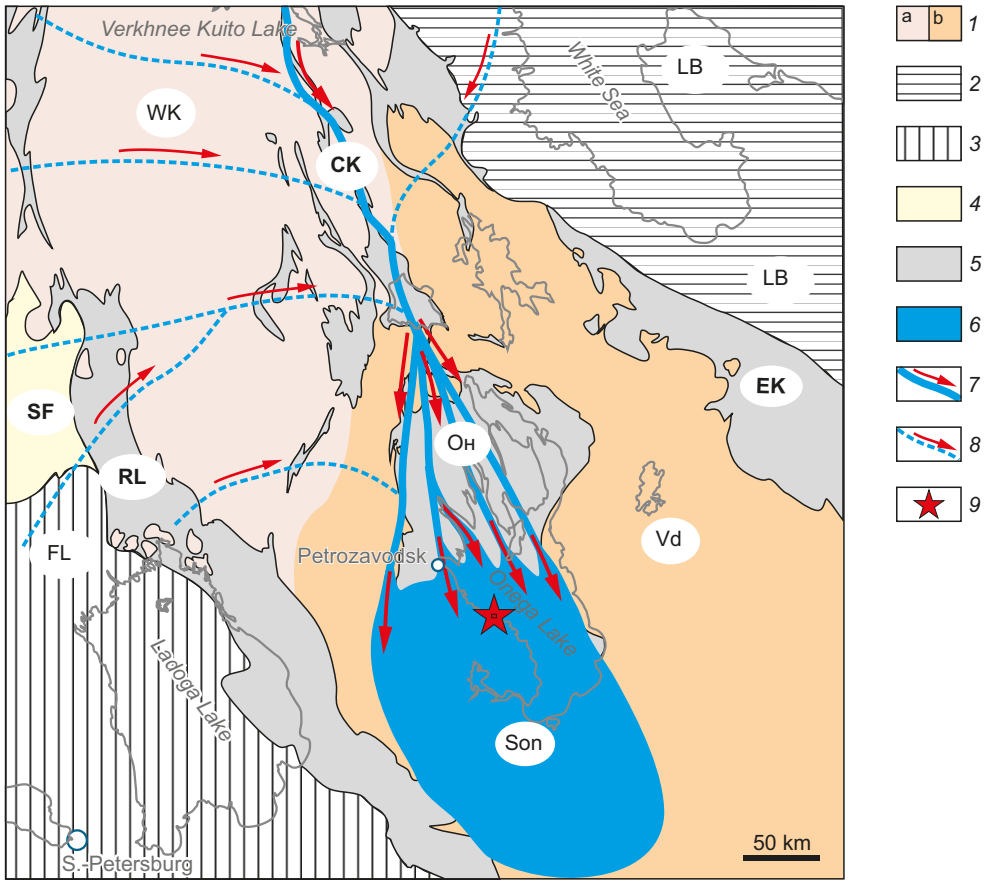

Fig. 11. Paleogeographic scheme of the southeastern part of the Baltic Shield for the Late Vepsian time.
1 – Archean granite-greenstone complexes: a – of the West Karelian (WK), б – of the Vodlozersk (Vd) massifs; *2* – Archean – Lower Proterozoic granulite-gneiss complexes of the Lapland-White Sea belt (LB); *3–5* – Lower Proterozoic complexes: *3* – metamorphic and igneous of the South Finnish-Ladoga belt (FL), *4* – volcanogenic-sedimentary and magmatic island-arcs of the Svekofennian accretionary orogen (SF), *5* – volcanogenic-sedimentary riftogenic and marginal-continental of the Karelian massif; *6* – South Onega basin of accumulation of terrigenous sediments; *7–8* – sedimentation flows and directions of material transportation: *7* – main, *8* – secondary; *9* – place of sampling KL-555. Tectonic zones: RL – Raakh-Ladoga, CK – Central Karelian, EK – East Karelian; On – North Onega synclinorium, Son – South Onega sedimentation basin.

granulite and eclogite complexes (dZr transport distance 500–650 km). The main stream ran probably along the Central Karelian shear zone where the paleodrainage system that actually just might be on the site of the modern Lake Verkhnee Kuito was exhibited by 2310 Ma dolerite dykes (dZr transport distance 450 km) (Fig. 11). Moving further south-southeast along the weak fracture zone of central Karelia, the main stream might also pick up the Late Archean and Early Proterozoic detrital sediment. However, the largest number of fluvially transported dZr grains fell in the mouth of the stream within the North Onega synclinorium that had undergone the syn-Svecofennian (1.9–1.87 Ga) deformation before the Vepsian time. The dominant dZr groups in the age intervals 2.1–1.98 Ga, 2.05–2.08 Ga and 1.96–1.90 Ga appear to have been captured from the Lyudikovian basites (dZr transport distance 40–100 km). Some sedimentary evidence (cross-bedding, landslides) implies that detrital sediment was transported south and south-southeast. Therefore, the inland paleoriver delta was located in the area of the North Onega synclinorium (Fig. 11). This triangular-shaped space is like the modern Volga delta, with its numerous arms flowing into the Caspian Sea. The submarine delta and its related sediment wedge gradually prograded south into the South Onega trough.

With a limited significance of the secondary rewashing of sediments and dZr recycling it can be assumed that the main stream draining the area of the Central Karelian fracture zone was over 650 km in length. In case of more frequent occurrence of dZr recycling, the long sediment flow discussed above may be related to separate heterochronous fragments – more local drainage basins.

Since the age data sets for dZr grains from the rocks of the Ladoga Group are very similar to those for dZr grains from the Shoksha quartzite-sandstones (sample KL-555), it is believed that the Central Karelian main stream was fed by numerous right tributaries running through the Ladoga Group area within the Raakhe-Ladoga zone (Fig. 11). The assumption that these streams were not directly connected with the South Onega basin, but captured by the Central Karelian main stream is based on the structural and textural characteristics of the Shoksha quartzite-sandstones indicating the south-dominant direction of sediment transport. Otherwise, there could be observed east- and southeast-trending sediment transportation. The tributaries considered might have started from the areas of the Svecofennian accretionary orogen and South Finland-Ladoga metamorphic belt, with the zircon grains presumably captured from the granulite complexes (Fig. 11).

10. CONCLUSIONS

Obtained for the first time the U-Th-Pb ages for dZr grains from the Shoksha quartzite-sandstones in the South Onega trough, together with the previous isotope geochronology data on crystalline complexes of the southeastern Fennoscandia, allowed the following conclusions.

1. The weighted average of the three youngest U-Pb isotopic ages for dZr grains from red quartzite-sandstones of the Shoksha Formation is 1906±13 Ma that allows estimating the lower age limit on the formation-constituent sand sediment at about 1.91 Ga. In consideration of the previously obtained age of gabbrodolerites from the Ropruchei sill, cutting through the rocks of the Shoksha Formation, the occurrence time of the latter is confined to an interval 1.91–1.75 Ga, which covers a rather long (and uncertain) period lasted 150 Ma.

2. The Shoksha quartzite-sandstones are highly mature rocks consisting largely of quartzite that were formed under continental conditions due to predominantly north-northwest-to-east-southeast-directed sediment transportation.

3. The Shoksha quartzite-sandstones are formed due to accumulation of sediment deposited by streams which transported the Early Proterozoic and to a lesser extent Late Archean detrital material of crystalline complexes. The source area of the dominant dZr groups with age intervals 2.1–1.98 Ga (6 dates), 2.05–2.08 Ga (3 dates) and 1.96–1.90 Ga (18 dates) is most probably located within the Lyudikovian magmatic rocks (2100–1920 Ma) of the North Onega synclinorium and, perhaps, the rocks of the Ladoga Group widespread along the margin of the Svecofennian accretionary orogen.

4. The age data sets for dZr grains from the quartzite-sandstones of the Shoksha Formation and the rocks of the Ladoga Group are very similar to each other (coefficient p=0.27 of the Kolmogorov – Smirnov test) and characteristic mainly for tectono-magmatic events occurred immediately prior to the main stage of the Svecofennian tectogenesis (1.9–1.87 Ga).

5. Six single-grained zircons are of Late Archean age spanning from 2.8 to 2.5 Ga. Their age span correlates well with that obtained for granitoids penetrated by the Onega parametric borehole in the same-name structure basement. However, among the dZr, there were found no Early Archean grains which could originate from tonalites of the Vodlozero block. The causes that prevented eroded materials from being transported to the Vepsian South Onega basin remain unknown.

6. Five dZr grains have a very low Th/U ratio (Th/U <0.1). These dZr grains most likely originated from ultrahigh-pressure complexes, such as, for example, eclogites of the Belomorian-Lapland belt widespread in the areas of Salma, Kuru-Vaara and Gridino.

11. CONTRIBUTION OF THE AUTHORS

All authors made an equivalent contribution to this article, read and approved the final manuscript.

12. DISCLOSURE

The authors declare that they have no conflicts of interest relevant to this manuscript.

13. REFERENCES

Akhmedov A.M., Panova E.G., Krupenik V.A., Sveshnikova K.Yu., 2004. Early Proterozoic and Devonian Paleobasins in the Arid Junction Zone between the Baltic Shield and

Russian Platform. Saint Petersburg University Press, Saint Petersburg, 140 p. (in Russian) [Ахмедов А.М., Панова Е.Г., Крупеник В.А., Свешникова К.Ю. Аридные палеобассейны раннего протерозоя и девона зоны сочленения Балтийского щита и Русской платформы. СПб.: Изд-во СПбГУ, 2004. 140 с.].

Andersen T., 2002. Correction of Common Lead in U-Pb Analyses That Do Not Report ^{204}Pb. Chemical Geology 192 (1–2), 59–79. https://doi.org/10.1016/S0009-2541(02)00195-X.

Andersen T., 2008. ComPbCorr – Software for Common Lead Correction of U-Th-Pb Analyses That Do Not Report ^{204}Pb. In: P.J. Sylvester (Ed.), Laser Ablation ICP-MS in the Earth Sciences: Current Practices and Outstanding Issues. Mineralogical Association of Canada Short Course Series. Vol. 40. Vancouver, p. 312–314.

Andreichev V.L., Soboleva A.A., Gehrels G., 2014. U-Pb Dating and Provenance of Detrital Zircons from the Upper Precambrian Deposits of North Timan. Stratigraphy and Geological Correlation 22, 147–159. https://doi.org/10.1134/S0869593814020026.

Andreichev V.L., Soboleva A.A., Hourigan J.K., 2017. Results of U-Pb (LA-ICP-MS) Dating of Detrital Zircons from Terrigenous Sediments of the Upper Part of the Precambrian Basement of Northern Timan. Bulletin of Moscow Society of Naturalists. Geological Series 92 (1), 10–20 (in Russian) [Андреичев В.Л., Соболева А.А., Хоуриган Дж.К. Результаты U-Pb (LA-ICP-MS) датирования детритовых цирконов из терригенных отложений верхней части докембрийского фундамента Северного Тимана // Бюллетень МОИП. Отдел геологический. 2017. Т. 92. № 1. С. 10–20].

Andreichev V.L., Soboleva A.A., Khubanov V.B., Sobolev I.D., 2018. U-Pb (LA-ICP-MS) Age of Detrital Zircons from Meta-Sedimentary Rocks of the Upper Precambrian Section of Northern Timan. Bulletin of Moscow Society of Naturalists. Geological Series 93 (2), 14–26 (in Russian) [Андреичев В.Л., Соболева А.А., Хубанов В.Б., Соболев И.Д. U-Pb (LA-ICP-MS) возраст детритовых цирконов из метаосадочных пород основания верхнедокембрийского разреза Северного Тимана // Бюллетень МОИП. Отдел геологический. 2018. Т. 93. № 2. С. 14–26].

Berezin A.V., Travin V.V., Marin Y.B., Skublov S.G., Bogomolov E.S., 2012. New U-Pb and Sm-Nd Ages and P-T Estimates for Eclogitization in the Fe-Rich Gabbro Dyke in Gridino Area (Belomorian Mobile Belt). Doklady Earth Sciences 444, 760–765. https://doi.org/10.1134/S1028334X12060207.

Bibikova E.V., Kirnozova E.I., Lazarev Yu.N., Makarov V.A., Nikolaev A.A., 1990. U-Pb Isotopic Age for Vepsian Karelia. Doklady of the USSR Academy of Sciences 310 (1), 212–216 (in Russian) [Бибикова Е.В., Кирнозова Е.И., Лазарев Ю.Н., Макаров В.А., Николаев А.А. U-Pb изотопный возраст вепсия Карелии // Доклады АН СССР. 1990. Т. 310. № 1. С. 212–216].

Bibikova E., Petrova A., Claesson S., 2005a. The Temporal Evolution of the Sanukitoids in the Karelian Craton, Baltic Shield: An Ion Microprobe U-Th-Pb Isotopic Study of Zircons. Lithos 79 (1–2), 129–145. https://doi.org/10.1016/j.lithos.2004.05.005.

Bibikova E.V., Samsonov A.V., Petrova A.Yu., Kirnozova T.I., 2005b. The Archean Geochronology of Western Karelia. Stratigraphy and Geological Correlation 13 (5), 459–475.

Chekulaev V.P., Arestova N.A., Berezhnaya N.G., Presnyakov S.L., 2009a. New Data on the Age of the Oldest Tonalite-Trondhjemite Association in the Baltic Shield. Stratigraphy and Geological Correlation 17, 230–234. https://doi.org/10.1134/S0869593809020105.

Chekulaev V.P., Arestova N.A., Lobach-Zhuchenko S.B., Sergeev S.A., 2009b. Age of Dikes in Ancient Tonalites of the Vodlozero Terrane as the Key to Archean Evolution of Basic Magmatism of the Fennoscandian Shield. Doklady Earth Sciences 428, 1117. https://doi.org/10.1134/S1028334X09070174.

Daly J.S., Balagansky V.V., Timmerman M.J., Whitehouse M.J., 2006. The Lapland-Kola Orogen: Palaeoproterozoic Collision and Accretion of the Northern Fennoscandian Lithosphere. Geological Society London Memoirs 32, 579–598. https://doi.org/10.1144/GSL.MEM.2006.032.01.35.

Dokukina K.A., Kaulina T.V., Konilov A.N., Natapov L.M., Belousova E.A., Van K.V., Simakin S.G., Lepekhina E.N., 2014. Mesoarchean Mafic Dykes of the Belomorian Eclogite Province (Gridino Village Area, Russia). Doklady Earth Sciences 457, 824–830. https://doi.org/10.1134/S1028334X14070034.

Elhlou S., Belousova E., Griffin W.L., Pearson N.J., O'Reily S.Y., 2006. Trace Element and Isotopic Composition of GJ-Red Zircon Standard by Laser Ablation. Geochmica et Cosmochimica Acta 70 (18), A158. http://dx.doi.org/10.1016/j.gca.2006.06.1383.

Ershova V.B., Ivleva A.S., Podkovyrov V.N., Khudoley A.K., Fedorov P.V., Stockli D., Anfinson O., Maslov A.V., Khubanov V., 2019. Detrital Zircon Record of the Mesoproterozoic to Lower Cambrian Sequences of NW Russia: Implications for the Paleogeography of the Baltic Interior. GFF 141 (4), 279–288. https://doi.org/10.1080/11035897.2019.1625073.

Galdobina L.P., 1958. Jotnian Formations in Cis-Onega of the Karelian ASSR. Izvestiya of the Kola Branch of the USSR Academy of Sciences 1, 10–18 (in Russian) [Галдобина Л.П. Иотнийские образования района Прионежья Карельской АССР // Известия Карельского и Кольского филиалов АН СССР. 1958. № 5. С. 10–18].

Galdobina L.P., Mikhailyuk E.M., 1966. Lithology of Jotnian Formations in the Onega Syneclise. In: Problems of the Precambrian Sedimentary Geology. Iss. 1. Nedra, Moscow, p. 54–60 (in Russian) [Галдобина Л.П., Михайлюк Е.М. Литология иотнийских образований Онежской синеклизы // Проблемы осадочной геологии докембрия / Ред. А.В. Сидоренко. Вып. 1. М.: Недра, 1966. С. 54–60].

Galdobina L.P., Mikhailyuk E.M., 1971. Lithology and Paleogeography of the Middle Proterozoic Sediments in Karelia. In: Problems of the Precambrian Lithology. Leningrad, p. 21–31 (in Russia) [Галдобина Л.П., Михайлюк Е.М. Литология и палеогеография осадочных образований среднего

протерозоя Карелии // Проблемы литологии докембрия. Л., 1971. С. 21–31].

Garbar D.I., 1971. Stratigraphy. Upper Proterozoic. Jotnian Series. Upper Proterozoic (Post Jotnian) Magmatic Formations. In: Geology of the USSR. Leningrad, Pskov and Novgorod Regions. Vol. 1. Nedra, Moscow, p. 64–81 (in Russian) [Гарбар Д.И. Стратиграфия. Верхний протерозой. Йотнийская серия. Верхнепротерозойские (постиотнийские) магматические образования // Геология СССР. Ленинградская, Псковская и Новгородская области. М.: Недра, 1971. Т. 1. С. 64–81].

Glushanin L.V., Sharov N.V., Shchiptsov V.V. (Eds), 2011. Onega Paleoproterozoic Structure (Geology, Tectonics, Deep Structure and Minerageny). KSC RAS, Petrozavodsk, 431 p. (in Russian) [Онежская палеопротерозойская структура (геология, тектоника, глубинное строение и минерагения) / Ред. Л.В. Глушанин, Н.В. Шаров, В.В. Щипцов. Петрозаводск: КНЦ РАН, 2011. 431 с.].

Gorokhov I.M., Kuznetsov A.B., Melezhik V.A., Konstantinova G.V., Mel'nikov N.N., 1998. Sr Isotopic Composition in Upper Jatulian Dolomites of the Tulomozero Formation, South-Eastern Karelia. Doklady Earth Sciences 360 (3), 533–536.

Griffin W.L., Powell W.J., Pearson N.J., O'Reilly S.Y., 2008. GLITTER: Data Reduction Software for Laser Ablation ICPMS. In: P.J. Sylvester (Ed.), Laser Ablation ICP-MS in the Earth Sciences: Current Practices and Outstanding Issues. Mineralogical Association of Canada Short Course Series. Vol. 40. Vancouver, p. 308–311.

Guynn J., Gehrels G.E., 2010. Comparison of Detrital Zircon Age Distributions in the K-S Test. University of Arizona, Arizona LaserChron Center, Tucson, 16 p.

Harrison T.M., Watson E.B., Aikman A.B., 2007. Temperature Spectra of Zircon Crystallization in Plutonic Rocks. Geology 35 (7), 635–638. https://doi.org/10.1130/G23505A.1.

Heiskanen K.I., 1990. Paleogeography of the Baltic Shield in Karelian Time. KSC USSR Publishing House, Petrozavodsk, 126 p. (in Russian) [Хейсканен К.И. Палеогеография Балтийского щита в карельское время. Петрозаводск: Изд-во КНЦ АН СССР, 1990. 126 с.].

Heiskanen K.I., 1996. Early Proterozoic Sedimentary Basins of the Baltic Shield (Cross-Sectional Correlation, Reconstruction, Evolution). Brief PhD Thesis (Doctor of Geology and Mineralogy). Saint Petersburg, 64 p. (in Russian) [Хейсканен К.И. Раннепротерозойские седиментационные бассейны Балтийского щита (корреляция разрезов, реконструкции, эволюция): Автореф. дис. … докт. геол.-мин. наук. СПб., 1996. 64 с.].

Horstwood M.S.A., Kosler J., Gehrels G., Jackson S.E., McLean N.M., Paton Ch., Pearson N.J., Sircombe K., Sylvester P., Vermeesch P., Bowring J.F., Condon D.J., Schoene B., 2016. Community-Derived Standards for LA-ICP-MS U-(Th-)Pb Geochronology – Uncertainty Propagation, Age Interpretation and Data Reporting. Geostandards and Geoanalytical Research 40 (3), 311–332. https://doi.org/10.1111/j.1751-908X.2016.00379.x.

Hoskin P.W.O., Schaltegger U., 2003. The Composition of Zircon and Igneous and Metamorphic Petrogenesis. Reviews in Mineralogy and Geochemistry 53 (1), 27–62. https://doi.org/10.2113/0530027.

Hölttä P., Heilimo E., Huhma H., Kontinen A., Mertanen S., Mikkola P., Paavola J., Peltonen P., Semprich J., Slabunov A., Sorjonen-Ward P., 2014. The Archaean Karelia and Belomorian Provinces, Fennoscandian Shield. In: Y. Dilek, H. Furnes (Eds), Evolution of Archean Crust and Early Life. Modern Approaches in Solid Earth Sciences. Vol. 7. Springer, Dordrecht, p. 55–102. https://doi.org/10.1007/978-94-007-7615-9_3.

Jackson S.E., Pearson N.J., Griffin W.L., Belousova E., 2004. The Application of Laser Ablation Inductively Coupled Plasma-Mass Spectrometry to in situ U-Pb Zircon Geochronology. Chemical Geology 211 (1–2), 47–69. https://doi.org/10.1016/j.chemgeo.2004.06.017.

Kaczmarek M.A., Müntener O., Rubatto D., 2008. Trace Element Chemistry and U-Pb Dating of Zircons from Oceanic Gabbros and Their Relationship with Whole Rock Composition (Lanzo, Italian Alps). Contributions to Mineralogy and Petrology 155, 295–312. https://doi.org/10.1007/s00410-007-0243-3.

Kharitonov L.Ya., 1966. Structure and Stratigraphy of Karelides of the Eastern Baltic Shield. Nauka, Moscow, 360 p. (in Russian) [Харитонов Л.Я. Структура и стратиграфия карелид восточной части Балтийского щита. М.: Наука, 1966. 360 с.].

Kirkland C.L., Daly J.S., Whitehouse M.J., 2008. Basement-Cover Relationships of the Kalak Nappe Complex, Arctic Norwegian Caledonides and Constraints on Neoproterozoic Terrane Assembly in the North Atlantic Region. Precambrian Research 160 (3–4), 245–276. https://doi.org/10.1016/j.precamres.2007.07.006.

Kirkland C.L., Smithies R.H., Taylor R.J.M., Evans N., McDonald B., 2015. Zircon Th/U Ratios in Magmatic Environs. Lithos 212–215, 397–414. https://doi.org/10.1016/j.lithos.2014.11.021.

Kolodyazhny S.Yu., 2006. Structural and Kinematic Evolution of the South-Eastern Part of the Baltic Shield in the Paleoproterozoic. GEOS, Moscow, 332 p. (in Russian) [Колодяжный С.Ю. Структурно-кинематическая эволюция юго-восточной части Балтийского щита в палеопротерозое. М.: ГЕОС, 2006. 332 с.].

Kolodyazhny S.Yu., Zykov D.S., Leonov M.G., Orlov S.Yu., 2000. The Evolution of Dome- and Shear-Type Structural Features of Northwestern Onega Area Kareliya Rock Massif. Russian Journal of Earth Sciences 2 (2), 135–151. http://dx.doi.org/10.2205/2000ES000039.

Korosov V.I., 1991. Prejatulian Proterozoic Geology of the Eastern Baltic Shield (Sumian, Sariolian). KSC USSR Publishing House, Petrozavodsk, 118 p. (in Russian) [Коросов В.И. Геология доятулийского протерозоя восточной части Балтийского щита (сумий, сариолий). Петрозаводск: Изд-во КНЦ АН СССР, 1991. 118 с.].

Korsakov A.K., Mezhelovskaya S.V., Mezhelovsky A.D., 2015. Quartzites of the Tokshinskaya Formation (Proterozoic) of the Vetreny Belt: Composition, Conditions of Formation and Deformation. Bulletin of Moscow Society of Naturalists. Geological Series 90 (1), 7–17 (in Russian)

[Корсаков А.К., Межеловская С.В., Межеловский А.Д. Кварциты токшинской свиты (протерозой) Ветреного пояса: состав, условия образования и деформации // Бюллетень Московского общества испытателей природы. Отдел геологический. 2015. Т. 90. № 1. С. 7–17].

Korsman K., Korja T., Pajunen M., Virransalo P., GGT/SVEKA Working Group, 1999. The GGT/SVEKA Transect: Structure and Evolution of the Continental Crust in the Paleoproterozoic Svecofennian Orogen in Finland. International Geology Review 41 (4), 287–333. https://doi.org/10.1080/00206819909465144.

Kozhevnikov V.N., 2000. Archean Greenstone Belts of the Karelian Craton as Accreationary Orogens. KSC RAS, Petrozavodsk, 223 p. (in Russian) [Кожевников В.Н. Архейские зеленокаменные пояса Карельского кратона как аккреционные орогены. Петрозаводск: КНЦ РАН. 2000. 223 с.].

Kozhevnikov V.N., 2011. Hadean-Archaean Detrital Zircons – Tools for Understanding of the Ancient Geological History of Fennoscandian Shield. In: Geology of Karelia from the Archaean to the Present. Proceedings of the All-Russian Conference Convened to Celebrate the 50th Anniversary of the Founding of the Institute of Geology, Karelian Research Centre, RAS (May, 24–26 2011). KarRC RAS, Petrozavodsk, p. 37–48 (in Russian) [Кожевников В.Н. Хадей-архейские детритовые цирконы – ключ к познанию древнейшей геологической истории Фенноскандинавского щита // Геология Карелии от архея до наших дней: Материалы докладов Всероссийской конференции, посвященной 50-летию Института геологии КарНЦ РАН (24–26 мая 2011 года). Петрозаводск: КарНЦ РАН. 2011. С. 37–48].

Kozhevnikov V.N., Berezhnaya N.G., Presnyakov S.L., Lepekhina E.N., Antonov A.V., Sergeev S.A., 2006. Geochronology (SHRIMP II) of Zircons from Archean Stratotectonic Associations of Karelian Greenstone Belts: Significance for Stratigraphic and Geodynamic Reconstructions. Stratigraphy and Geological Correlation 14, 240–259. https://doi.org/10.1134/S0869593806030026.

Kozhevnikov V.N., Medvedev P.V., Skublov S.G., Marin Y.B., Systra Y., Valencia V., 2010. Hadean-Archean Detrital Zircons from Jatulian Quartzites and Conglomerates of the Karelian Craton. Doklady Earth Sciences 431, 318–323. https://doi.org/10.1134/S1028334X10030128.

Kozhevnikov V.N., Skublov S.G., 2010. Detritic Zircons from the Archean Quartzites of the Matlakhta Greenstone Belt of the Karelian Craton: Hydrothermal Alterations, Mineral Inclusions, and Isotope Age. Doklady Earth Sciences 430, 223–227. https://doi.org/10.1134/S1028334X10020170.

Krats K.O., 1955. On Some Problems of Proterozoic Geology and Baltic Field Structure. Proceedings of the Laboratory of Precambrian Geology of the USSR Academy of Sciences 5, 175–188 (in Russian) [Кратц К.О. О некоторых вопросах геологии протерозоя и строении Балтийского щита // Труды лаборатории геологии докембрия АН СССР. 1955. Вып. 5. С. 175–188].

Krats K.O., 1963. Geology of Karelides of Karelia. Publishing House of the USSR Academy of Sciences, Moscow, Leningrad, 209 p. (in Russian) [Кратц К.О. Геология карелид Карелии. М.-Л.: Изд-во АН СССР, 1963. 209 с.].

Kulikov V.S. (Ed.), 1999. The Proterozoic Suisar' Picrite-Basalt Complex in Karelia (Key Section and Petrology). KarRS RAS, Petrozavodsk, 96 p. (in Russian) [Суйсарский пикрит-базальтовый комплекс палеопротерозоя Карелии (опорный разрез и петрология) / Ред. В.С. Куликов. Петрозаводск: КарНЦ РАН, 1999. 96 с.].

Kulikov V.S., Kulikova V.V., 2014. On Development of the Lower Precambrian Stratigraphic Scale of Russia. In: Geology and Mineral Resources of Karelia. Vol. 17. KarRC RAS, Petrozavodsk, p. 25–28 (in Russian) [Куликов В.С., Куликова В.В. К созданию Российской национальной стратиграфической шкалы нижнего докембрия // Геология и полезные ископаемые Карелии. Петрозаводск: КарНЦ РАН, 2014. Вып. 17. С. 25–28].

Kulikov V.S., Kulikova V.V., Polin A.K., 2017a. New Chronostratic Scheme of South-Eastern Fennoscandia and Its Use in the Preparation of Small-Scale Geological Maps of the Precambrian Regions. Proceedings of Higher Educational Establishments. Geology and Exploration 5, 5–12 (in Russian) [Куликов В.С., Куликова В.В., Полин А.К. Новая хроностратиграфическая схема Юго-Восточной Фенноскандии и ее использование при составлении мелкомасштабных геологических карт докембрийских регионов // Известия высших учебных заведений. Геология и разведка. 2017. № 5. С. 5–12].

Kulikov V.S., Simon A.K., Kulikova V.V., Samsonov A.V., Kairyak A.I., Ganin V.A., Zudin A.I., 1990. The Archean Evolution of Magmatism of the Vodlozero Block of the Karelian granite-greenstone area. In: Precambtian Geology and Geochronology of the East European Platform. Nauka, Leningrad, p. 92–100 (in Russian) [Куликов В.С., Симон А.К., Куликова В.В., Самсонов А.В., Кайряк А.И., Ганин В.А., Зудин А.И. Эволюция магматизма Водлозерского блока Карельской гранит-зеленокаменной области в архее // Геология и геохронология докембрия Восточно-Европейской платформы. Л.: Наука, 1990. С. 92–100].

Kulikov V.S., Svetov S.A., Slabunov A.I., Kulikova V.V., Polin A.K., Golubev A.I., Gorkovets V.Ya., Ivashchenko V.I., Gogolev M.A., 2017b. Geological Map of Southeastern Fennoscandia in Scale 1:750000: A New Approach to Map Compilation. Iss. 2. Proceedings of KSC RAS, p. 3–41 (in Russian) [Куликов В.С., Светов С.А., Слабунов А.И., Куликова В.В., Полин А.К., Голубев А.И., Горьковец В.Я., Иващенко В.И., Гоголев М.А. Геологическая карта Юго-Восточной Фенноскандии масштаба 1:750000: новые подходы к составлению // Труды КНЦ РАН. 2017. № 2. С. 3–41]. https://doi.org/10.17076/geo444.

Kuptsova A.V., Khudoley A.K., Davis W., Rainbird R.H., Kovach V.P., Zagornaya N.Y., 2011. Age and Provenances of Sandstones from the Riphean Priozersk and Salmi Formations in the Eastern Pasha-Ladoga Basin (Southern Margin of the Baltic Shield). Stratigraphy and Geological Correlation 19, 125–140. https://doi.org/10.1134/S0869593811020067.

Kuznetsov A.B., Gorokhov I.M., Azimov P.Y., Dubinina E.O., 2021. Sr- and C- Chemostratigraphy Potential of

the Paleoproterozoic Sedimentary Carbonates under Medium-Temperature Metamorphism: The Ruskeala Marble, Karelia. Petrology 29, 175–194. https://doi.org/10.1134/S0869591121010033.

Kuznetsov A.B., Gorokhov I.M., Melezhik V.A., Mel'nikov N.N., Konstantinova G.V., Turchenko T.L., 2012. Strontium Isotope Composition of the Lower Proterozoic Carbonate Concretions: The Zaonega Formation, Southeast Karelia. Lithology and Mineral Resources 47, 319–333. https://doi.org/10.1134/S0024490212030066.

Kuznetsov A.B., Gorokhov I.M., Melnikov N.N., Konstantinova G.V., Kutyavin E.P., Turchenko T.L., Melezhik V.A., 2010. Sr Isotopic Composition of Paleoproterozoic 13C-Rich Carbonate Rocks: The Tulomozero Formation, SE Fennoscandian Shield. Precambrian Research 182 (4), 300–312. https://doi.org/10.1016/j.precamres.2010.05.006.

Kuznetsov A.B., Gorokhov I.M., Ovchinnikova G.V., Melezhik V.A., Vasil'eva I.M., Gorokhovskii B.M., Konstantinova G.V., Mel'nikov N.N., 2011. Rb-Sr and U-Pb Systematics of Metasedimentary Carbonate Rocks: The Paleoproterozoic Kuetsjarvi Formation of the Pechenga Greenstone Belt, Kola Peninsula. Lithology and Mineral Recourses 46, 151–164. https://doi.org/10.1134/S0024490211020040.

Kuznetsov N.B., Baluev A.S., Terekhov E.N., Kolodyazhnyi S.Yu., Przhiyalgovskii E.S., Romanyuk T.V., Dubensky A.S., Sheshukov V.S., Lyapunov S.M., Bayanova T.B., Serov P.A., 2021. Time Constraints on the Formation of the Kandalaksha and Keretsk Grabens of the White Sea Paleo-Rift System from New Isotopic Geochronological Data. Geodynamics & Tectonophysics 12 (3), 570–607 (in Russian) [Кузнецов Н.Б., Балуев А.С., Терехов Е.Н., Колодяжный С.Ю., Пржиялговский Е.С., Романюк Т.В., Дубенский А.С., Шешуков В.С., Ляпунов С.М., Баянова Т.Б., Серов П.А. О времени формирования Кандалакшского и Керецкого грабенов палеорифтовой системы Белого моря в свете новых данных изотопной геохронологии // Геодинамика и тектонофизика. 2021. Т. 12. № 3. С. 570–607]. https://doi.org/10.5800/GT-2021-12-3-0540.

Kuznetsov N.B., Natapov L.M., Belousova E.A., O'Reilly S.Y., Griffin W.L., 2010a. Geochronological, Geochemical and Isotopic Study of Detrital Zircon Suites from Late Neoproterozoic Clastic Strata along the NE Margin of the East European Craton: Implications for Plate Tectonic Models. Gondwana Research 17 (2–3), 583–601. https://doi.org/10.1016/j.gr.2009.08.005.

Kuznetsov N.B., Natapov L.M., Belousova E.A., O'Relly S.Y., Kulikova K.V., Soboleva A.A., Udoratina O.V., 2010b. The First Results of the Dating (U/Pb) and Isotopic-Geochemistry Study of the Detrital Zircons from the Neoproterozoic Sandstones of the Southern Timan (Djejim-Parma Hill). Doklady Earth Sciences 435, 1676–1683. https://doi.org/10.1134/S1028334X10120263.

Kuznetsov N.B., Romanyuk T.V., Belousova E.A., 2018. The First Results of U-Pb Isotope Dating of Detrital Zircons from the Upper Mesoproterozoic Gulliksenfellet Quartzite (Southern Part of Wedel Jarlsberg Land, Southwest Spitsbergen). Doklady Earth Sciences 479, 305–309. https://doi.org/10.1134/S1028334X18030194.

Lahtinen R., Huhma H., 2019. A Revised Geodynamic Model for the Lapland-Kola Orogen. Precambrian Research 330, 1–19. https://doi.org/10.1016/j.precamres.2019.04.022.

Larin A.M., 2009. Rapakivi Granites in the Geological History of the Earth. Part 1, Magmatic Associations with Rapakivi Granites: Age, Geochemistry, and Tectonic Setting. Stratigraphy and Geological Correlation 17, 235. https://doi.org/10.1134/S0869593809030010.

Larin A.M., 2011. Rapakivi Granites and Associated Rocks. Nauka, Saint Petersburg, 402 p. (in Russian) [Ларин А.М. Граниты рапакиви и ассоциирующие породы. СПб.: Наука, 2011. 402 с.].

Leonov M.G., Kolodyazhnyi S.Yu., Somin M.L., 1995. Tectonic Flow Structures in the Deposits of the Proto-platform Cover of the Karelian Massif. Bulletin of Moscow Society of Naturalists. Geological Section 70 (3), 20–32 (in Russian) [Леонов М.Г., Колодяжный С.Ю., Сомин М.Л. Структуры тектонического течения в отложениях протоплатформенного чехла Карельского массива // Бюллетень МОИП. Отдел геологический. 1995. Т. 70. № 3. С. 20–32].

Levchenkov O.A., Lobach-Zhuchenko S.B., Sergeev S.A., 1989. Geochronology of the Karelian Granite-Greenstone Area. In: L.K. Levskii, O.A. Levchenkov, Precambrian Isotope Chronology. Nauka, Leningrad, p. 63–72 (in Russian) [Левченков О.А., Лобач-Жученко С.Б., Сергеев С.А. Геохронология Карельской гранит-зеленокаменной области // Изотопная геохронология докембрия / Ред. Л.К. Левский, О.А. Левченков. Л.: Наука, 1989. С. 63–72].

Linnemann U., Ouzegane K., Drareni A., Hofmann M., Becker S., Gärtner A., Sagawe A., 2011. Sands of West Gondwana: An Archive of Secular Magmatism and Plate Interactions – A Case Study from the Cambro-Ordovician Section of the Tassili Ouan Ahaggar (Algerian Sahara) Using U-Pb-LA-ICP-MS Detrital Zircon Ages. Lithos 123 (1–4), 188–203. https://doi.org/10.1016/j.lithos.2011.01.010.

Lobach-Zhuchenko S.B., Chekulaev V.P., Arestova N.A., Levskii L.K., Kovalenko A.V., 2000. Archean Terranes in Karelia: Geological and Isotopic–Geochemical Evidence. Geotectonics 34 (6), 452–466.

Lobach-Zhuchenko S.B., Glebovitskii V.A., Arestova N.A., 2009. Mantle Sources of Rocks in the Vodlozero Domain of the Fennoscandian Shield. Doklady Earth Sciences 429, 1284. https://doi.org/10.1134/S1028334X09080108.

Lobach-Zhuchenko S.B., Sergeev S.A., Levchenkov O.A., Ovchinnikova G.V., Kotova L.N., Krylov I.N., Yakovleva S.Z., 1989. The Archean Vodlozero Gneiss Complex and Its Structural-Metamorphic Evolution. In: Precambrian Isotope Geochronology. Nauka, Leningrad, p. 14–44 (in Russian) [Лобач-Жученко С.Б., Сергеев С.А., Левченков О.А., Овчинникова Г.В., Котова Л.Н., Крылов И.Н., Яковлева С.З. Водлозерский гнейсовый комплекс раннего архея и его структурно-метаморфическая эволюция // Изотопная геохронология докембрия. Л., 1989. С. 14–44].

Lower Precambrian Stratigraphic Scale of Russia, 2002. Explanatory Note. KarRS RAS, Apatity, 13 p. (in Russian) [Общая стратиграфическая шкала нижнего докембрия России: Объяснительная записка. Апатиты: КНЦ РАН, 2002. 13 с.].

Lubnina N.V., Pisarevsky S.A., Söderlund U., Nilsson M., Sokolov S.J., Khramov A.N., Iosifidi A.G., Ernst R., Romanovskaya M.A., Pisakin B.N., 2012. New Palaeomagnetic and Geochronological Data from the Ropruchey Sill (Karelia, Russia): Implications for Late Palaeoproterozoic Palaeogeography. In: S. Mertanen, L.J. Pesonen, P. Sangchan (Eds), Supercontinent Symposium 2012 (Sept. 25–28, 2012). Programme and Abstracts. Geological Survey of Finland, p. 81–82.

Lubnina N.V., Slabunov A.I., 2017. The Karelian Craton in the Structure of the Kenorland Supercontinent in the Neoarchean: New Paleomagnetic and Isotope Geochronology Data on Granulites of the Onega Complex. Moscow University Geology Bulletin 72, 377–390. https://doi.org/10.3103/S0145875217060072.

Ludwig K.R., 2012. ISOPLOT 3.75. A Geochronological Toolkit for Microsoft Excel. User's Manual. Berkeley Geochronology Center Special Publication 5, 75 p.

Makarikhin V.V., Kononova G.M., 1983. The Lower Proterozoic Phytoliths of Karelia. Nauka, Leningrad, 180 p. (in Russian) [Макарихин В.В., Кононова Г.М. Фитолиты нижнего протерозоя Карелии. Л.: Наука, 1983. 180 с.].

Makarikhin V.V., Medvedev P.V., Satsuk Yu.I., 1995. Subdivision and Correlation of the Jatulian of the Stratotypical Area (Lower Proterozoic Karelia). In: Outlines of Precambrian Geology of Karelia. IG KarRS RAS, Petrozavodsk, p. 72–83 (in Russian) [Макарихин В.В., Медведев П.В., Сацук Ю.И. Расчленение и корреляция ятулия стратотипической местности (нижний протерозой Карелии) // Очерки геологии докембрия Карелии. Петрозаводск: ИГ КарНЦ РАН, 1995. С. 72–83].

Martin A.P., Prave A.R., Condon D.J., Lepland A., Fallick A.E., Romashkin A.E., Medvedev P.V., Rychanchik D.V., 2015. Multiple Palaeoproterozoic Carbon Burial Episodes and Excursions. Earth and Planetary Science Letters 424, 226–236. https://doi.org/10.1016/j.epsl.2015.05.023.

Mezhelovskaya S.V., Korsakov A.K., Mezhelovskii A.D., Bibikova E.V., 2016. Age Range of Formation of Sedimentary-Volcanogenic Complex of the Vetreny Belt (The Southeast of the Baltic Shield). Stratigraphy and Geological Correlation 24, 105–117. https://doi.org/10.1134/S0869593816020040.

Mikhailenko Yu.V., 2016. Structural Features and Composition of the Karuyarva Formation, Kildin Group of Ripheids, Sredny Peninsula (Northern Framing of the Kola Peninsula). PhD Thesis (Candidate of Geology and Mineralogy). Ukhta, 205 p. (in Russian) [Михайленко Ю.В. Особенности строения и состав каруярвинской свиты кильдинской серии рифеид полуострова Средний (северное обрамление Кольского полуострова): Дис. … канд. геол.-мин. наук. Ухта, 2016. 205 с.].

Mikhailenko Yu.V., Soboleva A.A., Hourigan J.K., 2016. U-Pb Age of Detrital Zircons from Upper Precambrian Deposits of the Sredni and Rybachi Peninsulas (Northern Margin of the Kola Peninsula). Stratigraphy and Geological Correlation 24, 439–463. https://doi.org/10.1134/S086959381605004X.

Miller Yu.V., 1988. Structure of Archean Greenstone Belts. Nauka, Leningrad, 144 p. (in Russian) [Миллер Ю.В. Структура архейских зеленокаменных поясов. Л.: Наука, 1988. 144 с.].

Mints M.V., Berzin R.G., Suleimanov A.K., Zamozhnyaya N.G., Stupak V.M., Konilov A.N., Zlobin V.L., Kaulina T.V., 2004. The Deep Structure of Early Precambrian Crust of the Karelian Craton, Southeastern Fennoscandian Shield: Results of Investigation along CMP PROFILE 4B. Geotectonics 2, 10–29 (in Russian) [Минц М.В., Берзин Р.Г., Сулейманов А.К., Заможняя Н.Г., Ступак В.М., Конилов А.Н., Злобин В.Л., Каулина Т.В. Глубинное строение раннедокембрийской коры Карельского кратона, юго-восток Фенноскандинавского щита: результаты исследований вдоль профиля МОГТ 4В // Геотектоника. 2004. № 2. С. 10–29].

Mints M.V., Dokukina K.A., 2020. The Belomorian Eclogite Province (Eastern Fennoscandian Shield, Russia): Meso-Neoarchean or Late Paleoproterozoic? Geodynamics & Tectonophysics 11 (1), 151–200 (in Russian) [Минц М.В., Докукина К.А. Субдукционные эклогиты Беломорской эклогитовой провинции (восток Фенноскандинавского щита, Россия): мезоархей, неоархей или поздний палеопротерозой? // Геодинамика и тектонофизика. 2020. Т. 11. № 1. С. 151–200]. https://doi.org/10.5800/GT-2020-11-1-0469.

Mints M.V., Eriksson P.G., 2016. Secular Changes in Relationships between Plate-Tectonic and Mantle-Plume Engendered Processes during Precambrian Time. Geodynamics & Tectonophysics 7 (2), 173–232 (in Russian) [Минц М.В., Эрикссон П.Г. Длиннопериодные изменения в соотношении процессов тектоно-плитного и мантийно-плюмового происхождения в докембрии // Геодинамика и тектонофизика. 2016. Т. 7. № 2. С. 173–232]. https://doi.org/10.5800/GT-2016-7-2-0203.

Morozov A.F. (Ed.), 2010. Deep Structure, Evolution and Mineral Resources of the Early Precambrian Basement of the East European Platform: Interpretation of Materials for Profiles 1-EB, 4B and TATSES. Vol. 2. Iss. 4. GEOKART, GEOS, Moscow, 400 p. (in Russian) [Глубинное строение, эволюция и полезные ископаемые раннедокембрийского фундамента Восточно-Европейской платформы: Интерпретация материалов по опорному профилю 1-ЕВ, профилям 4В и ТАТСЕЙС / Ред. А.Ф. Морозов. М.: ГЕОКАРТ, ГЕОС, 2010. Т. 2. Вып. 4. 400 с.].

Negrutsa V.Z., 1984. Early Proterozoic Stages of Development of the Eastern Baultic Shield. Nedra, Leningrad, 270 p. (in Russian) [Негруца В.З. Раннепротерозойские этапы развития восточной части Балтийского щита. Л.: Недра, 1984. 270 с.].

Negrutsa V.Z., 2011. Stratigraphy Aspects of the Lower Precambrian in Russia (Historical-Methodological Analysis). Lithosphere 1, 3–19 (in Russian) [Негруца В.З. Проблемы стратиграфии нижнего докембрия России (историко-методологический анализ) // Литосфера. 2011. № 1. С. 3–19].

Nikishin A.M., Romanyuk T.V., Moskovskii D.V., Kuznetsov N.B., Kolesnikova A.A., Dubenskii A.S., Sheshukov V.S., Lyapunov S.M., 2020. Upper Triassic Sequences of the Crimean Mountains: First Results of U-Pb Dating of Detrital Zircons.

Moscow University Geology Bulletin 75, 220–236. https://doi.org/10.3103/S0145875220030096.

Nironen M., 1997. The Svecofennian Orogen: A Tectonic Model. Precambrian Research 86 (1–2), 21–44. https://doi.org/10.1016/S0301-9268(97)00039-9.

Ovchinnikova G.V., Matrenichev G.V., Levchenkov O.A., Sergeev S.A., Yakovlev S.Z., Gorokhovsky B.M., 1994. U-Pb and Pb-Pb Isotope Dating of the Acid Volcanites from the Khautavaar Greenstone Structure, Central Karelia. Petrology 2 (3), 266–281 (in Russian) [Овчинникова Г.В., Матреничев В.А., Левченков О.А., Сергеев С.А., Яковлев С.З., Гороховский Б.М. U-Pb и Pb-Pb изотопные исследования кислых вулканитов Хаутаваарской зеленокаменной структуры, Центральная Карелия // Петрология. 1994. Т. 2. № 3. С. 266–281].

Paszkowski M., Budzyń B., Mazur S., Sláma J., Shumlyanskyy L., Środoń J., Dhuime B., Kędzior A., Liivamägi S., Pisarzowska A., 2019. Detrital Zircon U-Pb and Hf Constraints on Provenance and Timing of Deposition of the Mesoproterozoic to Cambrian Sedimentary Cover of the East European Craton, Belarus. Precambrian Research 331, 105352. https://doi.org/10.1016/j.precamres.2019.105352.

Perevozchikova V.A., 1957. Proterozoic Geology of Karelia. In: Collection of Materials on Geology and Mineral Resources of the Northwestern Part of the USSR. Iss. 1. Gosgeotechizdat, Leningrad, p. 35–52 (in Russian) [Перевозчикова В.А. Геология протерозоя Карелии // Материалы по геологии и полезным ископаемым северо-запада СССР. Л.: Госгеолтехиздат, 1957. Вып. 1. С. 35–52].

Petrov G.A., 2017. Geology of Pre-Paleozoic Complexes of the Middle Part of the Ural Mobile Belt. PhD Thesis (Doctor of Geology and Mineralogy). Saint Petersburg, 319 p. (in Russian) [Петров Г.А. Геология допалеозойских комплексов средней части Уральского подвижного пояса: Дис. … докт. геол.-мин. наук. СПб., 2017. 330 с.].

Polekhovsky Yu.S., Tarasova M.P., Nesterov A.R., 1995. Noble-Metal Mineralization of Complex-Ore Deposits within the Precambrian Black Schists of Zaonega Formation, Karelia. In: S.I. Rybakov, A.I. Golubev (Eds), Abstracts of the Regional Symposium "Noble Metals and Diamonds of the northern European Russia" and Scientific-Practical Conference "The Problems of Development of Mineral Resource Base of Platinum Metals in Russia". KarRC RAS, Petrozavodsk, p. 85–87 (in Russian) [Полеховский Ю.С., Тарасова М.П., Нестеров А.Р. Благороднометалльная минерализация месторождений комплексных руд в докембрийских черных сланцах Заонежья Карелии // Тезисы докладов регионального симпозиума «Благородные металлы и алмазы севера европейской части России» и научно-практической конференции «Проблемы развития минерально-сырьевой базы платиновых металлов России» / Ред. С.И. Рыбаков, А.И. Голубев. Петрозаводск: КарНЦ РАН, 1995. С. 85–87].

Priyatkina N.S., Khudoley A.K., Ustinov V.N., Kullerud K., 2014. 1.92 Ga Kimberlitic Rocks from Kimozero, NW Russia: Their Geochemistry, Tectonic Setting and Unusual Field Occurrence. Precambrian Research 249, 162–179. https://doi.org/10.1016/j.precamres.2014.05.009.

Puchtel I.S., Arndt N.T., Hofmann A.W., Haase K.M., Kröner A., Kulikov V.S., Kulikova V.V., Garbe-Schönberg C.-D., Nemchin A.A., 1998. Petrology of Mafic Lavas within the Onega Plateau, Central Karelia: Evidence for 2.0 Ga Plume-Related Continental Crustal Growth in the Baltic Shield. Contributions to Mineralogy and Petrology 130, 134–153. https://doi.org/10.1007/s004100050355.

Puchtel I.S., Zhuravlev D.Z., Ashikhmina N.A., 1992. Sm-Nd Age of the Suisar Formation of the Baltic Shield. Doklady of the USSR Academy of Sciences 326 (4), 706–711 (in Russian) [Пухтель И.С., Журавлев Д.З., Ашихмина Н.А. Sm-Nd возраст суйсарской свиты Балтийского щита // Доклады АН СССР. 1992. Т. 326. № 4. С. 706–711].

Puchtel I.S., Zhuravlev D.Z., Kulikova V.V., Samsonov A.V., Simon A.K., 1991. Komatiites of the Vodlozero Block (Baltic Shield). Doklady of the USSR Academy of Sciences 317 (1), 197–202 (in Russian) [Пухтель И.С., Журавлев Д.З., Куликова В.В. Коматииты Водлозерского блока (Балтийский щит) // Доклады АН СССР. 1991. Т. 317. № 1. С. 197–202].

Ramo O.T., Mänttäri I., Vaasjoki M., Upton B.G.J., Sviridenko L., 2001. Age and Significance of Mesoproterozoic CFB Magmatism, Lake Ladoga Region, NW Russia. In: Boston 2001: A Geo-Odyssey (November 1–10, 2001). GSA Annual Meeting and Exposition Abstracts. Geological Society of America, Boulder, Colorado, p. A139.

Romanyuk T.V., Kuznetsov N.B., Belousova E.A., Gorozhanin V.M., Gorozhanina E.N., 2018. Paleotectonic and Paleogeographic Conditions for the Accumulation of the Lower Riphean Ai Formation in the Bashkir Uplift (Southern Urals): The TerraneChrone® Detrital Zircon Study. Geodynamics & Tectonophysics 9 (1), 1–37 (in Russian) [Романюк Т.В., Кузнецов Н.Б., Белоусова Е.А., Горожанин В.М., Горожанина Е.Н. Палеотектонические и палеогеографические обстановки накопления нижнерифейской айской свиты Башкирского поднятия (Южный Урал) на основе изучения детритовых цирконов методом «TerraneChrone®» // Геодинамика и тектонофизика. 2018. Т. 9. № 1. С. 1–37]. https://doi.org/10.5800/GT-2018-9-1-0335.

Romanyuk T.V., Maslov A.V., Kuznetsov N.B., Belousova E.A., Ronkin Yu.L., Krupenin M.T., Goroganin V.M., Goroganina E.N., Seregina E.S., 2013. First Data on LA-ICP-MS U/Pb Zircon Geochronology of Upper Riphean Sandstones of the Bashkir Anticlinorium (South Urals). Doklady Earth Sciences 452, 997–1000. https://doi.org/10.1134/S1028334X13100164.

Rubatto D., 2017. Zircon: The Metamorphic Mineral. Reviews in Mineralogy and Geochemistry 83 (1), 261–295. https://doi.org/10.2138/rmg.2017.83.9.

Ryazantsev P.A., 2012. An Integrated Geophysical Profile across the Ropruchei Gabbrodolerite Sill on the Rzhanoe – Anashkino Segment. Transactions of Karelian Research Centre of RAS 3, 165–171 (in Russian) [Рязанцев П.А. Комплексный геофизический профиль через Ропручейский силл габбродолеритов на участке Ржаное – Анашкино // Труды Карельского научного центра РАН. 2012. № 3. С. 165–171].

Ryazantsev P.A., 2014. Geological Nature of Gravity and Magnetic Anomalies within the South Onega Trough. In: Geology and Mineral Resources of Karelia. Iss. 17. Publishing House of the Karelian Research Centre of the RAS, Petrozavodsk, p. 110–117 (in Russian) [Рязанцев П.А. Геологическая природа аномалий магнитного и гравитационного поля в пределах Южно-Онежской мульды // Геология и полезные ископаемые Карелии. Петрозаводск: Изд-во КарНЦ РАН, 2014. Вып. 17. С. 110–117].

Samsonov A.V., Berzin R.G., Zamozhnyaya N.G., Shchipansky A.A., Bibikova E.V., Kirnozova T.I., Konilov A.N., 2001. Processes of Formation of the Early Cambrian Rocks in Northwestern Karelia, Baltic Shield: Results of Geological, Petrological and Deep Seismic Sounding (Profile 4B) Studies. In: Crustal Deep Structure and Evolution of the Southeastern Fennoscandian Shield: Kem – Kalevala Profile. KarRC RAS, Petrozavodsk, p. 109–143 (in Russian) [Самсонов А.В., Берзин Р.Г., Заможняя Н.Г., Щипанский А.А., Бибикова Е.В., Кирнозова Т.Н., Конилов А.Н. Процессы формирования раннедокембрийской коры северо-запада Карелии, Балтийский щит: результаты геологических, петрологических и глубинных сейсмических (профиль 4В) исследований // Глубинное строение и эволюция земной коры восточной части Фенноскандинавского щита: профиль Кемь – Калевала. Петрозаводск: Изд-во КарНЦ РАН, 2001. С. 109–143].

Samsonov A.V., Spiridonov V.A., Larionova Y.O., Larionov A.N., 2016. The Central Russian Fold Belt: Paleoproterozoic Boundary of Fennoscandia and Volgo-Sarmatia, the East European Craton. In: The 32nd Nordic Geological Winter Meeting (January 13–15, 2016, Helsinki, Finland). Abstracts. Bulletin of the Geological Society of Finland (Spec. Vol.), p. 162.

Sergeev S.A., Berezhnaya N.G., 1985. Isotopic and Mineralogical Studies of Zircons from Granite-Gneiss Complex Midstream of the Vodla River (Southeastern Karelia). In: L.K. Levskii, O.A. Levchenkov (Eds), Data on Modern Isotope Chemistry and Cosmochemistry. Nauka, Leningrad, p. 118–124 (in Russian) [Сергеев С.А., Бережная Н.Г. Изотопно-минералогические исследования цирконов из гранитогнейсового комплекса пород района среднего течения р. Водла (Юго-Восточная Карелия) // Современные данные изотопной геохимии и космохимии / Ред. Л.К. Левский, О.А. Левченков. Л.: Наука, 1985. С. 118–124].

Sergeev S.A., Bibikova E.V., Levchenkov O.A., Lobach-Zhuchenko S.B., Yakovleva S.Z., Ovchinnikova G.V., Neimark L.A., Komarov A.N., Gorokhovsky B.M., 1990. Isotope Geochronology of the Vodlozero Gneiss Complex. Geochemistry 1, 73–83 (in Russian) [Сергеев С.А., Бибикова Е.В., Левченков О.А., Лобач-Жученко С.В., Яковлева С.З., Овчинникова Г.В., Неймарк Л.А., Комаров А.Н., Гороховский Б.М. Изотопная геохронология Водлозерского гнейсового комплекса // Геохимия. 1990. № 1. С. 73–83].

Sergeev S.A., Bibikova E.V., Matukov D.I., Lobach-Zhuchenko S.B., 2007. Age of the Magmatic and Metamorphic Processes in the Vodlozero Complex, Baltic Shield: An Ion Microprobe (SHRIMP II) U-Th-Pb Isotopic Study of Zircons. Geochemistry International 45, 198–205. https://doi.org/10.1134/S0016702907020097.

Sharov N.V. (Ed.), 2020. Proterozoic Ladoga Structure (Geology, Deep Structure and Minerageny Genesis). Publishing House of the Karelian Research Centre of the RAS, Petrozavodsk, 435 p. (in Russian) [Ладожская протерозойская структура (геология, глубинное строение и минерагения) / Ред. Н.В. Шаров. Петрозаводск: Изд-во КарНЦ РАН, 2020. 435 с.].

Shcherbak N.P., Gorkovets V.Ya., Dodatko A.D., Krestin E.M., Pap A.M., Skorzhinskaya T., Snezhko A.M., Strueva O.M., Fomenko V.Yu., Shchegolev I.N., 1986. Correlation Scheme for Stratigraphic Subdivisions of the Precambrian Ferruginous-Siliceous Formations in the European Part of the USSR. Geologicheskii Zhurnal 46 (2), 5–17 (in Russian) [Щербак Н.П., Горьковец В.Я., Додатко А.Д., Крестин Е.М., Пап А.М., Скоржинская Т., Снежко А.М., Струева О.М., Фоменко В.Ю., Щеголев И.Н. Схема корреляции стратиграфических подразделений железисто-кремнистых формаций докембрия европейской части СССР // Геологический журнал. 1986. Т. 46. № 2. С. 5–17].

Shumlyanskyy L., Hawkesworth C., Billström K., Bogdanova S., Mytrokhyn O., Romer R., Dhuime B., Claesson S. et al., 2017. The Origin of the Palaeoproterozoic AMCG Complexes in the Ukrainian Shield: New U-Pb Ages and Hf Isotopes in Zircon. Precambrian Research 292, 216–239. https://doi.org/10.1016/j.precamres.2017.02.009.

Shumlyanskyy L., Hawkesworth C., Dhuime B., Billström K., Claesson S., Storey C., 2015. $^{207}Pb/^{206}Pb$ Ages and Hf Isotope Composition of Zircons from Sedimentary Rocks of the Ukrainian Shield: Crustal Growth of the South-Western Part of East European Craton from Archaean to Neoproterozoic. Precambrian Research 260, 39–54. https://doi.org/10.1016/j.precamres.2015.01.007.

Simanovich I.M., 1966. Epigenesis and Early Stages in Metamorphism of the Shoksha Quartzite-Sandstones. Proceedings of the Geological Institute of the USSR Academy of Science. Iss. 153. Nauka, Moscow, 143 p. (in Russian) [Симанович И.М. Эпигенез и начальный метаморфизм шокшинских кварцитопесчаников // Труды ГИН АН СССР. М: Наука, 1966. Вып. 153. 143 с.].

Simanovich I.M., 1978. Guartz Sand Rock. Proceedings of the Geological Institute of the USSR Academy of Science. Iss. 314. Nauka, Moscow, 155 p. (in Russian) [Симанович И.М. Кварц песчаных пород // Труды ГИН АН СССР. М.: Наука, 1978. Вып. 314. 155 с.].

Sirotkin A.N., Marin Y.B., Kuznetsov N.B., Korobova G.A., Romanyuk T.V., 2017. The Age of Spitsbergen Basement Consolidation: U-Pb Dating of Detrital Zircons from the Upper Precambrian and Lower Carboniferous Clastic Rocks of the Northwestern Part of Nordenskiöld Land. Doklady Earth Sciences 477, 1282–1286. https://doi.org/10.1134/S1028334X17110253.

Skublov S.G., Astaf'ev B.Yu., Marin Yu.B., Berezin A.V., Mel'nik A.E., Presnyakov S.L., 2011. New Data on the Age of Eclogites from the Belomorian Mobile Belt at Gridino Settlement Area. Doklady Earth Sciences 439, 1163. https://doi.org/10.1134/S1028334X11080290.

Slabunov A.I., Balagansky V.V., Shchipansky A.A. (Eds), 2019. Early Precambrian Eclogites of the Belomorian Province, Fennoscandian Shield. Field Guidebook. KarRC RAS, Petrozavodsk, 81 p.

Sláma J., Košler J., Condon D.J., Crowley J.L., Gerdes A., Hanchar J.M., Horstwood M.S.A., Morris G.A. et al., 2008. Plešovice Zircon – A New Natural Reference Material for U-Pb and Hf Isotopic Microanalysis. Chemical Geology 249 (1–2), 1–35. https://doi.org/10.1016/j.chemgeo.2007.11.005.

Smolkin V.F., Mezhelovskaya S.V., Mezhelovsky A.D., 2020. The Sources of the Clastic Material of the Terrigenous Sequences of the Neoarchean and Paleoproterozoic Paleobasins in the Eastern Part of the Fennoscandian Shield Based on Isotope Analysis Data for Detrital Zircons (SIMS, LA-ICP-MS). Stratigraphy and Geological Correlation 28, 571–602. https://doi.org/10.1134/S086959382006009X.

Smolkin V.F., Sharkov E.V., 2009. Ancient Zircons (3.8 Ga) in the Early Proterozoic Volcanites of the East Karelia as Evidence of the Existence of the Early Archean Crust. In: Geology, History. Theory and Practice. Abstracts of the International Conference Dedicated to the 250th Anniversary of the Vernadsky State Geological Museum RAS (September 14–16, 2009). SGM RAS, Moscow, p. 232–234 (in Russian) [Смолькин В.Ф., Шарков Е.В. Древний циркон (3.8 млрд лет) в раннепротерозойских вулканитах Восточной Карелии как свидетельство существования раннеархейской коры // Геология: история, теория, практика: Тезисы докладов международной конференции, посвященной 250-летию Государственного геологического музея им. В.И. Вернадского РАН (14–16 сентября 2009 г.). М.: ГГМ РАН, 2009. С. 232–234].

Soboleva A.A., Andreichev V.L., Burtsev I.N., Nikulova N.Yu., Khubanov V.B., Sobolev I.D., 2019. Detrital Zircons from the Upper Precambrian Rocks of the Vym Group of the Middle Timan (U-Pb Age and Sources of Drift). Bulletin of Moscow Society of Naturalists. Geological Section 94 (1), 3–16 (in Russian) [Соболева А.А., Андреичев В.Л., Бурцев И.Н., Никулова Н.Ю., Хубанов В.Б., Соболев И.Д. Детритовые цирконы из верхнедокембрийских пород вымской серии Среднего Тимана (U-Pb возраст и источники сноса) // Бюллетень МОИП. Отдел геологический. 2019. Т. 94. Вып. 1. С. 3–16].

Sokolov V.A. (Ed.), 1984. Precambrian Stratigraphy of the Karelian ASSR (Archean, Lower Proterozoic). Karelian Branch of the AS USSR, Petrozavodsk, 115 p. (in Russian) [Стратиграфия докембрия Карельской АССР (архей, нижний протерозой) / Ред. В.А. Соколов. Петрозаводск: КарФ АН СССР, 1984. 115 с.].

Sokolov V.A. (Ed.), 1987. Geology of Karelia. Nauka, Leningrad, 231 p. (in Russian) [Геология Карелии / Ред. В.А. Соколов. Л.: Наука, 1987. 231 с.].

Sokolov V.A., Galdobina L.P., Ryleev A.V., Satsuk Yu.I., Svetov A.P., Heiskanen K.I., 1970. Geology, Lithology and Paleogeography of the Yatulian Rocks of the Central Karelia. Karelia Publishing House, Petrozavodsk, 366 p. (in Russian) [Соколов В.А., Галдобина Л.П., Рылеев А.В., Сацук Ю.И., Светов А.П., Хейсканен К.И. Геология, литология и палеогеография ятулия Центральной Карелии. Петрозаводск: Карелия, 1970. 366 с.].

Stepanova A.V., Salnikova E.B., Samsonov A.V., Egorova S.V., Stepanov V.S., 2020. Mafic Intrusions of ca. 2400 Ma Large Igneous Province in the Belomorian Mobile Belt: First Baddeleyite U-Pb ID-TIMS Data. Doklady Earth Sciences 493, 617–620. https://doi.org/10.1134/S1028334X20080218.

Stepanova A.V., Salnikova E.B., Samsonov A.V., Larionova Yu.O., Egorova S.V., Savatenkov V.M., 2017. The 2405 Ma Doleritic Dykes in the Karelian Craton: A Fragment of a Paleoproterozoic Large Igneous Province. Doklady Earth Sciences 472, 72–77. https://doi.org/10.1134/S1028334X17010196.

Stepanova A.V., Samsonov A.V., Larionov A.N., 2014a. The Final Stage of the Middle Proterozoic Magmatism in the Onega Structure: Data for Dolerites of Zaonega. Transactions of KarRC RAS 1, 3–16 (in Russian) [Степанова А.В., Самсонов А.В., Ларионов А.Н. Заключительный эпизод магматизма среднего палеопротерозоя в Онежской структуре: данные по долеритам Заонежья // Труды КарНЦ РАН. 2014. №1. С. 3–16].

Stepanova A.V., Samsonov A.V., Salnikova E.B., Puchtel I.S., Larionova Yu.O., Larionov A.N., Stepanov V.S., Shapovalov Y.B., Egorova S.V., 2014b. Palaeoproterozoic Continental MORB-Type Tholeiites in the Karelian Craton: Petrology, Geochronology, and Tectonic Setting. Journal of Petrology 55 (9), 1719–1751. https://doi.org/10.1093/petrology/egu039.

Stepanyuk L.M., Kurylo S.I., Dovbush T.I., Grinchenko O.V., Syomka V.O., Bondarenko S.M., Shumlyanskyy L.V., 2017. Geochronology of Granitoids of the Easterm Part of the Ingul Region (the Ukrainian Shield). Geochemistry and Ore Formation 38, 3–13. https://doi.org/10.15407/gof.2017.38.003.

Svetov A.P., 1979. Platform Basaltic Volcanism of the Karelian Karelides. Nauka, Leningrad, 208 p. (in Russian) [Светов А.П. Платформенный базальтовый вулканизм карелид Карелии. Л.: Наука, 1979. 208 с.].

Svetov S.A., Golubev A.I., Stepanova A.V., Kulikov V.S., Gogolev M.A., 2015. Archean and Paleoproterozic Complexes of the Central Karelia: Geological Excursion on the Route Petrozavodsk City – Konchezero Lake – Marcial Waters Health Resort – Girvas Rural Settlement – Koikary Village – Kivach Falls – Petrozavodsk City. In: Current Problems of Precambrian Geology, Geophysics and Geoecology. Materials of the XXVI Youth Scientific School-Conference Dedicated to the Memory of K.O. Krats, Corresponding Member of the AS USSR, and F.P. Mitrofanov, Academician of the RAS (October 12–16, 2015). KRC RAS, Petrozavodsk, p. 157–191 (in Russian) [Светов С.А., Голубев А.И., Степанова А.В., Куликов В.С., Гоголев М.А. Архейские и палеопротерозойские комплексы Центральной Карелии: Геологическая экскурсия по маршруту г. Петрозаводск – оз. Кончезеро – п. Марциальные воды – п. Гирвас – д. Койкары – вод. Кивач – г. Петрозаводск // Актуальные проблемы геологии докембрия, геофизики и геоэкологии: Материалы XXVI молодежной научной школы-конференции,

посвященной памяти чл.-корр. АН СССР К.О. Кратца и академика РАН Ф.П. Митрофанова (12–16 октября 2015 г.). Петрозаводск: КНЦ РАН, 2015. С. 157–191].

Systra Yu.Y., 1991. Tectonics of the Karelian Region. Nauka, Saint Petersburg, 176 p. (in Russian) [Сыстра Ю.Й. Тектоника Карельского региона. СПб.: Наука, 1991. 176 с.].

Teipel U., Eichhorn R., Loth G., Rohrmuller J., Holl R., Kennedy A., 2004. U-Pb SHRIMP and Nd Isotopic Data from the Western Bohemian Massif (Bayerischer Wald, Germany): Implications for Upper Vendian and Lower Ordovician Magmatism. International Journal of Earth Sciences 93, 782–801. https://doi.org/10.1007/s00531-004-0419-2.

Timofeev V.M., 1935. Petrography of Karelia. Petrography of the USRR. Series 1. Regional Petrography. Publishing House of the USSR Academy of Science, Moscow, Leningrad, 256 p. (in Russian) [Тимофеев В.М. Петрография Карелии. Петрография СССР. Серия 1. Региональная петрография. М.-Л.: Изд-во АН СССР, 1935. 256 с.].

Travin V.V., 2015. The Structural Position and Age of Eclogite Rocks in the Area of Gridino Village in the Belomorian Mobile Belt. Geotectonics 49, 425–438. https://doi.org/10.1134/S0016852115050064.

Udoratina O.V., Burtsev I.N., Nikulova N.Yu., Khubanov V.B., 2017. Age of Upper Precambrian Metasandstones of Chetlas Group of Middle Timan on U-Pb Dating of Detrital Zircons. Bulletin of Moscow Society of Naturalists. Geological Section 92 (5), 15–32 (in Russian) [Удоратина О.В., Бурцев И.Н., Никулова Н.Ю., Хубанов В.Б. Возраст метапесчаников верхнедокембрийской четласской серии Среднего Тимана на основании U-Pb датирования детритных цирконов // Бюллетень МОИП. Отдел геологический. 2017. Т. 92. № 5. С. 15–32].

Vigdorchik V.M., Garbar D.I., Oganesova A.M., Kabakov A.G., 1968. Onega-Ladoga Isthmus (Geological Structure). In: Geological Guide to the Moscow Canal and V.I. Lenin Volga-Baltic Waterway. Nauka, Leningrad, p. 162–174 (in Russian) [Вигдорчик В.М., Гарбар Д.И., Оганесова А.М., Кабаков А.Г. Онежско-Ладожский перешеек (геологическое строение) // Геологический путеводитель по каналу им. Москвы и Волго-Балтийскому водному пути им. В.И. Ленина. Л.: Наука, 1968. С. 162–174].

Voitovich V.S., 1971. On the Nature of the Koikar Shear Zone of the Baltic Shield. Geotectonics 1, 33–42 (in Russian) [Войтович В.С. О природе Койкарской зоны дислокаций Балтийского щита // Геотектоника. 1971. № 1. С. 33–42].

Wanless V.D., Perfit M.R., Ridley W.I., Wallace P.J., Grimes C.B., Klein E.M., 2011. Volatile Abundances and Oxygen Isotopes in Basaltic to Dacitic Lavas on Mid-Ocean Ridges: The Role of Assimilation at Spreading Centers. Chemical Geology 287 (1–2), 54–65. https://doi.org/10.1016/j.chemgeo.2011.05.017.

Wiedenbeck M., Allé P., Corfu F., Griffin W.L., Meier M., Oberli F., Von Quadt A., Roddick J.C., Spiegel W., 1995. Three Natural Zircon Standards for U-Th-Pb, Lu-Hf, Trace Element and REE Analyses. Geostandards and Geoanalytical Research 19 (1), 1–23. https://doi.org/10.1111/j.1751-908X.1995.tb00147.x.

Wiedenbeck M., Hanchar J.M., Peck W.H., Sylvester P., Valley J., Whitehouse M., Kronz A., Morishita Y. et al., 2004. Further Characterisation of the 91500 Zircon Crystal. Geostandards and Geoanalytical Research 28 (1), 9–39. https://doi.org/10.1111/j.1751-908X.2004.tb01041.x.

Zhang W., Roberts D., Pease V., 2016. Provenance of Sandstones from Caledonian Nappes in Finnmark, Norway: Implications for Neoproterozoic–Cambrian Palaeogeography. Tectonophysics 691, 198–205. https://doi.org/10.1016/j.tecto.2015.09.001.

APPENDIX 1

Table 1.1. Lower Precambrian part of the Stratigraphic scale of Russia (after [Kulikov, Kulikova, 2014])

I			II			III
International geologic time scale			Stratigraphic scale of Russia (project, 2014)			Regional stratigraphic charts
EON	ERA	PERIOD and its lower age limit, Ma	EONOTHEM	ERATHEM	SYSTEM (?) and its lower age limit, Ma	SE Fennoscandia, SUB-HORIZON and its lower age limit, Ma
Proterozoic	Meso-protero-zoic	Calymmian, 1600	Proterozoic	Mesoproteozoic	1650	Hogland, 1650
	Paleoproterozoic	Statherian, 1800		Paleoproterozoic (Karelian)	Vepsian, 1860	Vepsian, 1800
		Orosirian, 2050			Kalevian, 1920	Kalevian, 1920
		Rhyacian, 2300			Ludicovian, 2075	Ludicovian, 2100
					Yatulian, 2290	Yatulian, 2300
		Siderian, 2500			Sariolian, 2370	Sariolian, 2400
					Sumian, 2505	Sumian, 2500
Archean	Neo-archean	2800	Archean	Neoarchean (?)	Emian, 2720	2650
					Vodian, 2800	2800
	Meso-archean	3200		Mesoarchean (Lopian)	Vesian, 2935	3000
					Erzian, 3150	3200
	Paleo-archean	3600		Paleoarchean (Komsa)	Skoltian, 3360	
					Chudian, 3580	3600
	Eoarchean	4000			Zyryan, 3795	3800
Hadean			Hadean			

Table 1.2. Results of U-Pb isotopic (LA-ICP-MS) dating of detrital zircon grains from the Shoksha Formation (sample KL-555), Cis-Onega

Order number	Analysis number in sample KL-555	Th, ppm	U, ppm	Th/U	Ratio measurements (corrected for common lead)					Age, Ma						D1	D2
					$^{207}Pb/^{235}U$	1σ	$^{206}Pb/^{238}U$	1σ	RHO	$^{207}Pb/^{206}Pb$	1σ	$^{207}Pb/^{235}U$	1σ	$^{206}Pb/^{238}U$	1σ		
1	a1	146	166	0.88	5.51504	0.0599	0.34331	0.0036	0.96	**1904**	11	1903	9	1903	17	0.0	0.1
2	a10	178	291	0.61	4.05093	0.0341	0.25055	0.0016	0.77	1915	6	1644	7	1441	8	14.1	32.9
3	a11-CENTER	126	137	0.92	5.11642	0.0595	0.31937	0.0033	0.89	**1899**	12	1839	10	1787	16	2.9	6.3
4	a12-CENTER	143	95	1.50	5.40708	0.0651	0.32579	0.0034	0.87	**1962**	12	1886	10	1818	17	3.7	7.9
5	a13-CENTER	163	146	1.12	6.28375	0.0687	0.35623	0.0036	0.93	**2070**	11	2016	10	1964	17	2.6	5.4
6	a14	205	357	0.57	5.67555	0.048	0.27631	0.0017	0.74	2334	7	1928	7	1573	9	22.6	48.4
7	a15	573	1325	0.43	0.93896	0.0138	0.07122	0.0005	0.44	1540	13	672	7	443	3	51.7	247.6
8	a16	302	469	0.64	2.88707	0.0252	0.17144	0.0011	0.73	1988	7	1379	7	1020	6	35.2	94.9
9	a17-RIM	128	167	0.76	6.48312	0.0703	0.37184	0.0038	0.94	**2049**	11	2044	10	2038	18	0.3	0.5
10	a18	123	335	0.37	3.01205	0.0277	0.1912	0.0012	0.68	1868	8	1411	7	1128	7	25.1	65.6
11	a19	297	504	0.59	4.78732	0.0417	0.20261	0.0013	0.74	2571	7	1783	7	1189	7	50.0	116.2
12	a2	112	177	0.63	3.52633	0.1178	0.21115	0.0018	0.26	1973	29	1533	26	1235	10	24.1	59.8
13	a20	208	2403	0.09	0.44247	0.0137	0.04604	0.0003	0.22	919	34	372	10	290	2	28.3	216.9
14	a21	72	113	0.64	11.71435	0.1251	0.49375	0.005	0.95	**2578**	10	2582	10	2587	22	–0.2	–0.3
15	a22-CORE	74	182	0.41	5.14262	0.0574	0.30766	0.0032	0.92	1975	11	1843	9	1729	16	6.6	14.2
16	a23	69	179	0.38	5.49178	0.0601	0.33362	0.0034	0.93	**1947**	11	1899	9	1856	16	2.3	4.9
17	a24	49	1851	0.03	0.9391	0.0123	0.05163	0.0003	0.49	2124	12	672	6	325	2	106.8	553.5
18	a25	233	1129	0.21	1.13334	0.0124	0.07394	0.0005	0.57	1819	10	769	6	460	3	67.2	295.4
19	a26-CORE	170	241	0.71	5.64159	0.0623	0.33349	0.0034	0.93	**1996**	11	1922	10	1855	16	3.6	7.6
20	a27-RIM	405	1250	0.32	6.05005	0.0404	0.25405	0.0016	0.91	2584	6	1983	6	1459	8	35.9	77.1
21	a28	414	2140	0.19	0.20457	0.012	0.02501	0.0002	0.14	579	69	189	10	159	1	18.9	264.2
22	a29	78	107	0.73	11.8755	0.1297	0.39461	0.004	0.93	2968	10	2595	10	2144	19	21.0	38.4
23	a3	174	979	0.18	5.72933	0.0616	0.35258	0.0037	0.97	**1924**	11	1936	9	1947	17	–0.6	–1.2
24	a30	69	211	0.33	5.62996	0.0631	0.33296	0.0034	0.91	**1995**	11	1921	10	1853	16	3.7	7.7
25	a31-CORE	105	131	0.80	5.88859	0.0493	0.34585	0.0022	0.75	**2007**	6	1960	7	1915	10	2.3	4.8
26	a32	31	98	0.31	5.78101	0.0617	0.34948	0.0036	0.95	**1956**	11	1944	9	1932	17	0.6	1.2
27	a33-CORE	181	154	1.17	5.30679	0.0567	0.327	0.0033	0.95	**1922**	11	1870	9	1824	16	2.5	5.4
28	a34-CORE	176	169	1.05	5.36735	0.0574	0.33237	0.0034	0.95	**1913**	11	1880	9	1850	16	1.6	3.4

Table 1.2 (continued)

Order number	Analysis number in sample KL-555	Th, ppm	U, ppm	Th/U	Ratio measurements (corrected for common lead)					Age, Ma						D1	D2
					$^{207}Pb/^{235}U$	1σ	$^{206}Pb/^{238}U$	1σ	RHO	$^{207}Pb/^{206}Pb$	1σ	$^{207}Pb/^{235}U$	1σ	$^{206}Pb/^{238}U$	1σ		
29	a35	413	622	0.66	2.1807	0.0264	0.1493	0.001	0.53	1731	10	1175	8	897	5	31.0	93.0
30	a36-CORE	192	133	1.44	5.86768	0.0635	0.34939	0.0036	0.94	**1983**	11	1956	9	1932	17	1.2	2.6
31	a37	582	1321	0.44	0.91919	0.0152	0.06432	0.0004	0.40	1690	15	662	8	402	3	64.7	320.4
32	a38	450	1922	0.23	0.56394	0.0104	0.04135	0.0003	0.37	1604	18	454	7	261	2	73.9	514.6
33	a39-CENTER	215	125	1.72	13.83002	0.1485	0.51673	0.0037	0.67	**2777**	7	2738	10	2685	16	2.0	3.4
34	a4	172	280	0.61	4.65014	0.0394	0.28822	0.0018	0.75	1911	6	1758	7	1633	9	7.7	17.0
35	a40	133	123	1.08	12.41778	0.1331	0.4826	0.0049	0.95	**2713**	10	2637	10	2539	21	3.9	6.9
36	a41	331	996	0.33	1.2298	0.0187	0.08696	0.0006	0.42	1671	14	814	9	538	3	51.3	210.6
37	a42	199	315	0.63	5.06514	0.0417	0.29851	0.0018	0.75	2001	6	1830	7	1684	9	8.7	18.8
38	a43-RIM	73	77	0.94	5.85887	0.0646	0.35373	0.0036	0.91	**1958**	12	1955	10	1952	17	0.2	0.3
39	a44	381	886	0.43	1.66639	0.0171	0.11586	0.0007	0.61	1702	9	996	7	707	4	40.9	140.7
40	a45-RIM	121	231	0.52	5.35466	0.0586	0.32985	0.0033	0.91	**1922**	11	1878	9	1838	16	2.2	4.6
41	a46	305	1112	0.27	1.03221	0.0153	0.07574	0.0005	0.42	1602	14	720	8	471	3	52.9	240.1
42	a47-RIM	139	139	1.00	5.64578	0.068	0.32635	0.0034	0.85	2036	12	1923	10	1821	16	5.6	11.8
43	a48-RIM	204	214	0.95	5.1593	0.0582	0.31427	0.0032	0.89	1942	12	1846	10	1762	15	4.8	10.2
44	a49	778	3654	0.21	0.17364	0.0087	0.01557	0.0001	0.15	1218	53	163	8	99.6	0.8	63.7	1122.9
45	a50	162	129	1.26	6.42803	0.0714	0.36205	0.0036	0.90	**2081**	11	2036	10	1992	17	2.2	4.5
46	a51	363	580	0.63	2.10786	0.0226	0.13852	0.0009	0.58	1805	9	1151	7	836	5	37.7	115.9
47	a52	177	246	0.72	5.54291	0.0578	0.34323	0.0034	0.94	**1913**	11	1907	9	1902	16	0.3	0.6
48	a53-RIM	82	111	0.74	5.66151	0.0486	0.34624	0.0021	0.71	**1935**	7	1926	7	1917	10	0.5	0.9
49	a54	304	82	3.72	5.59212	0.0598	0.3446	0.0034	0.93	**1922**	11	1915	9	1909	16	0.3	0.7
50	a55	505	906	0.56	1.07098	0.0202	0.09608	0.0006	0.34	1218	18	739	10	591	4	25.0	106.1
51	a56	576	2379	0.24	0.17625	0.0126	0.02407	0.0002	0.11	333	89	165	11	153	1	7.8	117.6
52	a57	191	287	0.67	7.27096	0.0564	0.26211	0.0016	0.80	2836	6	2145	7	1501	8	42.9	88.9
53	a58	131	125	1.04	11.24043	0.0951	0.38637	0.0026	0.78	2913	6	2543	8	2106	12	20.8	38.3
54	a59	314	3123	0.10	0.22153	0.0103	0.01559	0.0001	0.18	1680	45	203	9	99.7	0.8	103.6	1585.1
55	a5-RIM	68	139	0.49	5.80468	0.0449	0.34122	0.0021	0.81	**2006**	6	1947	7	1893	10	2.9	6.0
56	a6	488	1334	0.37	0.94309	0.0152	0.06632	0.0005	0.42	1681	15	675	8	414	3	63.0	306.0

Table 1.2 (continued)

Order number	Analysis number in sample KL-555	Th, ppm	U, ppm	Th/U	Ratio measurements (corrected for common lead)					Age, Ma						D1	D2
					$^{207}Pb/^{235}U$	1σ	$^{206}Pb/^{238}U$	1σ	RHO	$^{207}Pb/^{206}Pb$	1σ	$^{207}Pb/^{235}U$	1σ	$^{206}Pb/^{238}U$	1σ		
57	a60	169	4766	0.04	0.02883	0.0074	0.00393	0.000006	0.06	338	321	29	7	25.3	0.4	14.6	1236.0
58	a62	225	561	0.40	2.26933	0.0182	0.14754	0.0008	0.68	1825	8	1203	6	887	5	35.6	105.7
59	a63	31	155	0.20	5.98262	0.0571	0.35787	0.0031	0.92	**1975**	11	1973	8	1972	15	0.1	0.2
60	a64	1043	3175	0.33	0.47397	0.0081	0.02323	0.0001	0.35	2323	15	394	6	148	0.9	166.2	1469.6
61	a65	1073	1042	1.03	1.11455	0.0258	0.10257	0.0006	0.26	1167	23	760	12	629	4	20.8	85.5
62	a66	575	1270	0.45	1.05901	0.0136	0.07587	0.0004	0.45	1647	12	733	7	471	3	55.6	249.7
63	a67	236	141	1.67	6.91158	0.0795	0.34814	0.0021	0.53	2276	8	2100	10	1926	10	9.0	18.2
64	a68	181	55	3.30	5.11366	0.0543	0.31537	0.0028	0.84	**1920**	12	1838	9	1767	14	4.0	8.7
65	a69-CORE	735	886	0.83	5.65732	0.0545	0.35026	0.003	0.90	**1913**	11	1925	8	1936	14	–0.6	–1.2
66	a7	84	175	0.48	5.66573	0.062	0.34794	0.0036	0.95	**1928**	11	1926	9	1925	17	0.1	0.2
67	a70-CORE	64	172	0.37	4.66508	0.0304	0.28804	0.0015	0.80	1918	7	1761	5	1632	8	7.9	17.5
68	a71	141	218	0.65	5.50773	0.0521	0.34027	0.003	0.93	**1917**	11	1902	8	1888	14	0.7	1.5
69	a72	923	1431	0.64	0.49395	0.0167	0.05862	0.0004	0.18	643	39	408	11	367	2	11.2	75.2
70	a73	188	404	0.46	3.11499	0.0251	0.19703	0.0011	0.67	1875	8	1436	6	1159	6	23.9	61.8
71	a74	170	55	3.12	14.71022	0.147	0.54034	0.0049	0.91	**2805**	11	2797	9	2785	20	0.4	0.7
72	a75	47	62	0.75	12.13632	0.1201	0.47811	0.0043	0.91	**2690**	10	2615	9	2519	19	3.8	6.8
73	a76	89	63	1.42	9.36275	0.0959	0.40877	0.0037	0.89	2519	11	2374	9	2209	17	7.5	14.0
74	a77	176	4370	0.04	0.04098	0.0044	0.00155	0.00003	0.18	2756	87	41	4	10	0.2	310.0	27460.0
75	a78-RIM	43	1099	0.04	8.40885	0.0464	0.41373	0.0021	0.92	**2316**	6	2276	5	2232	10	2.0	3.8
76	a79	107	153	0.70	5.46242	0.0392	0.33291	0.0018	0.75	**1941**	6	1895	6	1852	9	2.3	4.8
77	a8	194	303	0.64	9.60113	0.0745	0.35857	0.0023	0.84	2778	6	2397	7	1975	11	21.4	40.7
78	a80	129	100	1.29	10.7693	0.1083	0.4733	0.0042	0.89	**2508**	11	2503	9	2498	19	0.2	0.4
79	a9	682	2079	0.33	0.32227	0.0109	0.02459	0.0002	0.23	1529	33	284	8	157	1	80.9	873.9

Table 1.3. Summary data on the sedimentary strata of the Upper and Middle Riphean of the NE part of the EEP and its framing, for which detrital zircon U-Pb dating was performed

Marking on Fig. 1	Original number of sample	Region, area	Formation	Rock	Age, Ma	References
Z01	K18-501	Tersky Coast of the White Sea	Tersky Formation	Red sandstones	Younger than 1145 Ma late Middle Riphean	[Kuznetsov N.B. et al., 2021]
Z04	202	North Timan region	Rumyanichnaya Formation, Barmin Group	Quartzite-sandstones	Late Riphean Early Proterozoic	[Andreichev et al., 2018]
Z05	234	North Timan region	Yambozero Formation, Barmin Group	Quartzite-sandstones	Late Riphean Early Neoproterozoic	[Andreichev et al., 2017]
Z06	380	North Timan region	Malochernoretsk Formation, Barmin Group	Quartzite-sandstones	Late Riphean Early Neoproterozoic	[Andreichev et al., 2014]
Z07	Sh-44	Near Ladoga Lake region	Priozersk Formation in the Shotkusa-1 well	Red sandstones	Middle Riphean Mesoproterozoic	[Ershova et al., 2019]
Z08	G1-15	Middle Timan	Svetlinskaya Formation, Chetlass Group	Quartz-feldspar metasandstones	Late Middle Riphean Late Mesoproterozoic	[Udoratina et al., 2017]
Z09	K1-15	Middle Timan	Vizingskaya Formation, Chetlass Group	Quartz-feldspar metasandstones	Late Middle Riphean Late Mesoproterozoic	[Udoratina et al., 2017]
Z10	MT-16-6	Middle Timan	Lunvozh Formation, Vym Group	Quartzite-sandstones	Late Middle Riphean Late Mesoproterozoic	[Soboleva et al., 2019]
Z11	K05-301	South Timan	Dzhezhim Formation	Red sandstones	Late Riphean Early Neoproterozoic	[Kuznetsov N.B. et al., 2010a, 2010b]
Z15	K12-057	South Ural	Lemeza sub-formation, Zilmerdak Group, Karatavian	Quartzite-sandstones	Late Riphean Early Neoproterozoic	[Romanyuk et al., 2013]
Z16	C-163-1	Wedel Jarlsberg Land, Southwest Spitsbergen Is., Svalbard Arhipellago	Sophiebogen Group	Muscovite quartzites	Late Riphean Early Neoproterozoic	[Sirotkin et al., 2017]
Z17	K07-091	Wedel Jarlsberg Land, Southwest Spitsbergen Is., Svalbard Arhipellago	Gulliksenfjellet	Quartzites	late Middle Riphean Late Mesoproterozoic	[Kuznetsov N.B. et al., 2018]
Z18	KK2	Sredny Peninsula	Kuyakan Formation, Volokovo Group	Quartz-feldspar sandstones	Late Riphean Cryogenian (800–630)	[Mikhailenko, 2016; Mikhailenko et al., 2016]
Z19	KJ4	Sredny Peninsula	Karujärve Formation, Kildin Group	Quartz-feldspar sandstones	Late Riphean Cryogenian (800–630)	[Mikhailenko, 2016; Mikhailenko et al., 2016]
Z20	ZP1	Sredny Peninsula	Zemlepakhta Formation, Kildin Group	Quartz-feldspar sandstones	Late Riphean Cryogenian (800–630)	[Mikhailenko, 2016; Mikhailenko et al., 2016]
Z21	LN3	Rybachy Peninsula	Lonskaya Formation, Eina Group	Quartz-feldspar sandstones	Late Riphean Tonian (800–1130)	[Mikhailenko, 2016]

Table 1.3 (continued)

Marking on Fig. 1	Original № of sample	Region, area	Formation	Rock	Age, Ma	References
Z22	CK285 CK291 CK293	Finnmarken Peninsula	Hjelmsoy Formation	Sandstones	Late Riphean 980–1030	[Kirkland et al., 2008]
Z23	CK040	Finnmarken Peninsula	Porsanger sandstone formation (Porsanger orogeny)	Sandstones	Late Riphean 840–910	[Kirkland et al., 2008]
Z24	LAN1	Varanger Peninsula	Landersfjord Formation, Laksefjord Group	Sandstones		[Zhang et al., 2016]
Z25	Vilch-5B	Belorussia	Belorussia Formation, Orsha Group	Quartz arenites	Older than the Glusk Formation	[Paszkowski et al., 2019]
Z26	Vilch-6A, Vilch-7A,	Belorussia	Glusk Formation, Viltchitsy Group	Sand-matrix tillites	>977±6 >1056±4 overlying the Orsha Group	[Paszkowski et al., 2019]

Table 1.4. Summary data on the early Middle Riphean and older sedimentary strata in the NE part of the EEP and its framing, for which detrital zircon U-Pb dating was performed

Marking on Fig. 1	Original № of sample	Region, area	Formation	Rock	Age, Ma	References
S00	KL-555	Western coast of Onega Lake	Shoksha Formation	Quartzites		The present paper
S01	ТК-12-01	Vetrenyy Poyas	Toksha Formation	Quartzites	>2437	[Korsakov et al., 2015; Mezhelovskaya et al., 2016]
S02	X-12, X-26, X-36, X-78, X-92	Southeast Ladoga region	Priozersk and Salmi Formations	Quartz-feldspar sandstones	Lower Riphean from 1530–1547 to1458	[Kuptsova et al., 2011]
S03	10403/1 091/1	North Ladoga region	Ladoga Group	Biotite schist	1880-1922	[Sharov, 2020]
S04	3976, 5883	Karelia	Volomskaya syncline, Onega synclinorium	Jatulian quartzite and sand-matrix of Jatulian conglomerates	2300–2100	[Kozhevnikov, 2011]
S05	5081	Middle Ural	Isherim Formation	Quartzite-sandstones	Middle Riphean 1150–1079	[Petrov, 2017]
S06	Vilch-2, Vilch-4	Belorussia	Pinsk Formation of the Belorussia Group	Sandstones	>1228 constraints for the Polissya Group	[Paszkowski et al., 2019]
S07	56/90-95 drill hole#56 (depth 68.8 m) near the village of Tykhodvizh	Ukraine	Polissya Group of the Middle and Upper Riphean, Romeyki Formation, Polytsy and Zhobryn Formations of the Upper Riphean	Quartz-feldspar (arkose) sandstone	1200–1000 1228±15	[Shumlyanskyy et al., 2015]
S08	СК276 СК279	Finnmarken Peninsula	Fagervik complex		1948–1796	[Kirkland et al., 2008]
S09	УГ-72 П-21 П-26 П-73	North Kola Peninsula	Uraguba-Titovka belt, Pechenga structure			[Smolkin et al., 2020]
S10	IFJ1	Varanger Peninsula	Conglomerates of the Gozavarri basal unit, Ifjord Formation			[Zhang et al., 2016]

Table 1.5. Results of the Kolmogorov – Smirnov test

Lithostratigraphic complexes (groups, formations)	S00(KL-555) Shoksha quartzite-sandstones (the present paper)	S03(10403/1, 091/1) Karelia, Ladoga Group	S06(Vilch-2, Vilch-4) Central EEP areas, Pinsk Formation, Belorussia Group	Z04(202) North Timan, Rumyanichnaya Formation, Barmin Group	Z11(K05-301) South Timan, Dzhezhim Formation	Z15(K12-057) South Ural, Lemeza sub-formation, Zilmerdak Formation	Z17(K07-091) Spitsbergen Island, Gulliksenfjellet Formation	Z24(LAN1) Varanger Peninsula, Landersfjord Formation
S00(KL-555) Shoksha quartzite-sandstones (the present paper)		**0.265**	**0.097**	0.000	0.039	0.000	**0.413**	0.000
S03 (10403/1, 091/1), Ladoga Group [Sharov, 2020]	**0.265**		0.000	0.000	0.003	0.000	**0.192**	0.000
S06 (Vilch-2, Vilch-4) Pinsk Formation, Belorussia Group, [Paszkowski et al., 2019]	**0.097**	0.000		0.000	0.001	0.000	0.002	0.000
Z04 (202) North Timan, Rumyanichnaya Formation, Barmin Group [Andreichev et al., 2018]	0.000	0.000	0.000		0.001	0.000	0.000	0.034
Z11 (K05-301) South Timan, Dzhezhim Formation [Kuznetsov N.B. et al., 2010a, 2010b]	0.039	0.003	0.001	0.001		0.001	**0.415**	0.000
Z15 (K12-057) South Ural, Lemeza sub-formation, Zilmerdak Formation [Romanyuk et al., 2013]	0.000	0.000	0.000	0.000	0.001		0.000	0.000
Z17 (K07-091) Spitsbergen Island, Gulliksenfjellet Formation [Kuznetsov N.B.et al., 2018]	**0.413**	**0.192**	0.002	0.000	**0.415**	0.000		0.000
Z24 (LAN1) Varanger Peninsula, Landersfjord Formation [Zhang et al., 2016]	0.000	0.000	0.000	0.034	0.000	0.000	0.000	

Note. The calculations have been executed using a program [Guynn, Gehrels, 2010] available in the public domain. The Kolmogorov – Smirnov test is used to determine whether two empirical distributions obey the same law or the resulting distribution obeys the proposed model. The standard significance level of the test is usually taken to be 95 %. If the value of the obtained mutual coefficient p exceeds the threshold value of 0.05, then the tested empirical distributions obey the same distribution law with a probability of 95 %. The *p* values greater than the accepted threshold value of 0.05 are highlighted in bold. See Fig. 1 for sampling sites, the names of formations/strata are given in App. 1, Tables 1.3 and 1.4.